Chemical Engineering Science 257 (2022) 117721

Contents lists available at ScienceDirect

Chemical Engineering Science

journal homepage: www.elsevier.com/locate/ces

The DuQMoGeM application to the numerical modeling of liquid-liquid columns

Khaled Athmani [a], Paulo Laranjeira da Cunha Lage [b], Abdelmalek Hasseine [a,*]

[a] Laboratory LAR-GHYDE, University of Biskra, BP 145 RP, Biskra 07000, Algeria
[b] Programa de Engenharia Química — COPPE, Universidade Federal do Rio de Janeiro, PO Box 68502, Rio de Janeiro, RJ 21941-972, Brazil

HIGHLIGHTS

- A multi-compartment population balance model was developed for an extraction column.
- Test problems with known analytical solutions were solved by the DuQMoGeM.
- Accurate regular moments and good distributions' approximations were obtained.
- A pilot plant Kühni column was modeled using the multi-compartment model.
- DuQMoGeM results agree well with the experimental data for the Kühni column.

ARTICLE INFO

Article history:
Received 27 November 2021
Received in revised form 22 February 2022
Accepted 9 May 2022
Available online 18 May 2022

Keywords:
Population balance
DuQMoGeM
Liquid-liquid dispersion
Numerical modeling

ABSTRACT

This work extended the dual quadrature method of generalized moments (DuQMoGeM) to solve the population balance model for the hydrodynamics of liquid-liquid extraction columns using a multi-compartment model that represents batch and continuous well-mixed extraction vessels as particular cases. This model can either represent the actual sections of a column or its spatial discretization that can use moment preserving schemes for the advection and dispersion of the generalized moment set. The DuQMoGeM results were compared to analytical solutions for batch and continuous well-mixed vessels and extraction columns, showing that it is accurate for predicting the evolution of the low order moments and the drop number distribution along with the column height. We also modeled a Kühni column for which the simulation accurately predicted the steady-state experimental holdup, encouraging the DuQMoGeM usage to solve the population balance equation for heterogeneous systems and different columns.

1. Introduction

In general, a liquid-liquid extraction system consists of two almost immiscible phases, with one dispersed in the form of fine droplets in the other continuous liquid phase. Several relevant properties of the dispersed phase come from the number density distribution that may change due to several mechanisms such as coalescence, breakage, and growth. However, the number density distribution evolution comes from solving a population balance equation. Consequently, population balance modeling is a powerful tool for predicting the dispersed phase behavior in liquid-liquid extraction equipment, such as columns and reactors (Ramkrishna, 2000). In this sense, many scientific papers accomplished modeling and simulation of liquid-liquid extraction columns by the population balance equation. It became essential for modeling multiphase flow, mainly when a strong coupling exists between the number density distribution and the phase velocity fields (Bart et al., 2020).

Mathematically, the population balance equation (PBE) is an integro-differential equation that is usually difficult enough to solve analytically. Therefore, it has solutions just for a few simple cases. Several researchers have developed numerical methods to find approximated solutions. A possible classification groups these methods into the following categories: methods of moments, stochastic methods, and discretization (or class) methods.

The most common discretization methods are the finite difference, finite element, and finite volume methods. They all discretize the domain of the internal coordinate (for instance, droplet diameter) (Bart et al., 2020; Su et al., 2009). Although straightforward and accurate for calculating the particle size distribution, they have

* Corresponding author.
E-mail addresses: khaled.athmani@univ-biskra.dz (K. Athmani), paulo@peq.coppe.ufrj.br (P. L. da C. Lage), a.hasseine@univ-biskra.dz (A. Hasseine).

https://doi.org/10.1016/j.ces.2022.117721
0009-2509/

Nomenclature

a	inverse of the residence time $[s^{-1}]$
A	column cross-section area $[m^2]$
$\mathscr{A}_{jkli}$	aggregation matrix for compartment j $[m^{k+i+l}]$
B	daughter drop conditional probability distribution $[m^{-1}]$
c	coefficient in polynomial approximation of $\tilde{n}$ $[m^{-k-3}]$
c_v	form factor [–]
C_1	collision frequency model parameter [–]
C_2	coalescence efficiency model parameter $[m^{-2}]$
d	drop diameter as internal variable $[m]$
d_0	mother drop diameter on breakage $[m]$
d_1, d_2	diameters of coalescing drops $[m]$
D	column diameter $[m]$
D_R	rotor diameter $[m]$
$\mathscr{D}_{ef}$	effective dispersion coefficient $[m^2/s]$
f	collision frequency $[m^3/s]$
F	advective-dispersive flux $[m^{-3}\ s^{-1}]$
g	breakage frequency $[s^{-1}]$
g_0	breakage frequency model parameter [–]
G	generic function
$\mathscr{G}$	gravitational acceleration $[m/s^2]$
h	column height $[m]$
h_j	compartment height $[m]$
H	breakage and coalescence source terms $[m^{-4}\ s^{-1}]$
$\mathscr{H}$	Heaviside step function [–]
J	number of compartments [–]
$\mathscr{J}$	Jacobian of the transformation of internal coordinates [–]
k_v	slowing factor [–]
$\mathscr{L}_{jki}$	breakage matrix for compartment j $[m^{i+k}/s]$
m	mean of the Gaussian distribution $[m]$
M	number of Gauss-Legendre quadrature points [–]
n	drop number distribution in d variable $[m^{-4}]$
n_{in}	normalized drop number distribution of the feed $[m^{-1}]$
$\tilde{n}$	drop number distribution in x variable $[m^{-3}]$
N_p	power number [–]
N_q	number of Gauss-Christoffel quadrature points [–]
N_R	rotor speed in revolutions per second $[s^{-1}]$
N_0	total number density of drops in the feed $[m^{-3}]$
$P(d)$	breakage probability [–]
$\mathscr{P}$	power input per compartment $[W]$
Q	phase volumetric flowrate $[m^3/s]$
r_d	dispersed phase fraction (hold-up) [–]
Re_R	Reynolds number of rotor/agitator [–]
s, u	drop diameter values $[m]$
S	source term $[m^{-4}\ s^{-1}]$
t	time $[s]$
t_h	hydrodynamic residence time $[s]$
v	phase velocity $[m/s]$
v_r	relative velocity $[m/s]$
v_t	terminal velocity $[m/s]$
V_d	compartment volume $[m^3]$
$\mathscr{V}_{jki}$	convection matrix for compartment j $[m^{k+i+1}/s]$
w	weight of the quadrature rule [–]
We_m	modified Weber number [–]
We_R	rotor Weber number [–]
x	dimensionless diameter coordinate [–]
Y	auxiliary variable
y, q	dimensionless diameter values [–]
z	height coordinate $[m]$
z_c	continuous feed inlet $[m]$
z_d	dispersed feed inlet $[m]$

Greek letters

α	standard deviation of the Gaussian distribution $[m]$
β	auxiliary function
$\delta(X)$	Dirac delta function $[X^{-1}]$
$\delta_{i,j}$	Kronecker delta
$\Delta\rho$	density difference between phases $[kg/m^3]$
Δz	height above disperse phase inlet, $z - z_d$ $[m]$
ϵ	mechanical power dissipation $[W/kg]$
ζ	dimensionless height variable, $\zeta = z/h$
η	dynamic viscosity $[Pa\ s]$
θ	plate free area fraction [–]
κ	exponent in the swarm effect factor [–]
λ	coalescence probability [–]
Λ	auxiliary function
$\mu_k^{(\phi)}$	generalized moment of order k using the ϕ polynomial family $[m^{k-3}]$
μ_k	regular moment of order k $[m^{k-3}]$
ν	mean number of daughter droplets [–]
ξ	abscissa of the quadrature rule [–]
ϖ	angular velocity $\varpi = 2\pi N_R$ $[s^{-1}]$
$\Pi_k^{(\phi)}$	moments of the daughter distribution function of order k $[m^k]$
ρ	density $[kg/m^3]$
σ	interfacial tension $[N/m]$
$\upsilon(d)$	drop volume corresponding to drop of diameter d $[m^3]$
$\upsilon'(d)$	derivative of drop volume function, $d\upsilon/d(d)$ $[m^2]$
$\bar{\upsilon}_{in}$	mean drop volume of the feed distribution $[m^3]$
Φ, Φ	auxiliary functions
$\phi_k(d)$	k-degree orthogonal polynomial in d variable $[m^k]$
$\varphi_k(x)$	k-degree orthogonal polynomial in terms of the x variable $[m^k]$
χ	auxiliary function
ψ	generic function
ω	coalescence frequency $[m^3/s]$
ω_0	coalescence frequency model parameter [–]

Subscripts

a	coalescence
b	breakage
c	continuous phase
$crit$	critical
d	dispersed phase
in	inlet
max	maximum
min	minimum

Superscripts

(a)	analytical solution
(ϕ)	relative to ϕ polynomial family
(φ)	relative to φ polynomial family

high computational costs to guarantee mass conservation (Bart et al., 2020). These methods can approximate the distribution function in each discretization interval by a unique value (zero-order methods) or use high-order polynomials (higher-order methods) (Bart et al., 2020).

Gelbard and Seinfeld (1978) applied the orthogonal collocation on finite elements to the population balance equation. Nicmanis and Hounslow (1996) solved a continuous crystallizer's steady-state population balance model using the Galerkin method and the orthogonal collocation methods on finite elements. Mantzaris et al. (2001a,b) used the finite difference and finite element meth-

ods to solve multivariate cell population balance models. Kumar and Ramkrishna (1996a,b, 1997) proposed three new approaches: the fixed pivot, the moving pivot, and the Lagrangian-moving pivot discretization methods. Campos and Lage (2003) simulated a bubble extraction column using the Lagrangian-moving pivot technique. Attarakih et al. (2004) developed the extended fixed pivot technique (EFPT) to solve the PBE describing the hydrodynamics of interacting liquid-liquid phases.

Hulburt and Katz (1964) introduced the method of moments. It has various advantages, such as efficiency, accuracy, and low computational cost, making it widely used to solve the PBE. On the other hand, it does not give an approximation for the particle number distribution (Bart et al., 2020). However, some mathematical techniques for reconstructing the size distribution function from its moments exist in the literature (John et al., 2007). One of the most famous moments methods is the quadrature method of moments. It was first introduced and applied by McGraw (1997) to describe the growth of aerosols and then extended to models with aggregation and breakage by Marchisio et al. (2003). The main idea behind this method is the approximation of the integrals by the Gaussian quadrature constructed from the number density distribution moments. Marchisio and Fox (2005) introduced the direct quadrature method of moments, whose central idea is the solution of transport equations for the quadrature weights and abscissas, avoiding their computation along the solution. Attarakih et al. (2006) introduced the sectional quadrature method of moments (SQMOM), which is a hybrid method involving the methods of classes and moments. The SQMOM discretizes the particle size domain in sections. The so-called primary particle represents the particle size in each one, being calculated from the secondary particles that are the abscissas of a local low-order quadrature. These local quadratures compute the breakage and coalescence terms.

The method of moments lacks a representation of the particle number distribution. Lage (2011) introduced the dual quadrature method of generalized moments that gives a series approximation for the number density distribution using an orthogonal polynomial family whose coefficients are related to the generalized moments of the distribution for this polynomial family. The usage of high-order fixed-point Gaussian quadratures based on the same polynomial family controls the accuracy of the integral terms. Santos et al. (2013) introduced the direct version of DuQMoGeM that solves transport equations for the weights and abscissas of the Gauss-Christoffel quadrature. Another method that provides an approximation for the distribution is the extended quadrature method of moments (EQMOM), introduced by Yuan et al. (2012). It represents the number density distribution by a series of kernel density functions (KDF) whose locations are the abscissas of the Gauss-Christoffel quadrature. The EQMOM employs secondary Gaussian quadratures based on the KDFs to control the solution accuracy.

This work applies the DuQMoGeM to solve the population balance equation for liquid-liquid columns using a multi-compartment model that represents a well-mixed vessel as a particular case. The multi-compartment model can either represent a discretization of a continuous contact column or a multiple-staged column. The model must use appropriate correlations for calculating the inter-compartment drop fluxes for a specific kind of extraction column. The calculation of spatial moment fluxes using DuQMoGeM has never been carried out before. Although several other methods can solve this problem, we did not intend to compare them to the DuQMoGeM in the present work. It must be pointed out that the DuQMoGeM was developed and tested previously only using the particle volume as the internal variable (Lage, 2011). As it has never been applied to solve problems using the particle diameter as the internal variable, we first applied it to solve such population balance models for test cases with analytical solutions. These include models for well-mixed reactors in both continuous and closed systems and a liquid-liquid extraction column without diffusion and with constant phase velocities. Finally, a realistic case of a Kühni column was modeled and solved, and the results were compared to available experimental data.

2. Population balance models

2.1. Model for a liquid-liquid extraction column

The population balance equation for the areal-averaged drop number distribution, $n(t,z,d)$, in a liquid-liquid extraction column can be written as (Ramkrishna, 2000; Kronberger et al., 1995):

$$\frac{\partial n(t,z,d)}{\partial t}+\frac{\partial F(t,z,d)}{\partial z}=S(t,z,d)+H(t,z,d) \tag{1}$$

where $z\in[0,h]$ is the vertical coordinate, being h the column height, and $d\in[d_{min},d_{max}]\subset[0,\infty]$ is the drop equivalent diameter, where d_{min} and d_{max} are physically imposed limits for the drop size distribution, that is, $n(t,z,d)=0,\forall d\notin[d_{min},d_{max}]$. We proceed in this section as if the extraction column is continuous, that is, without internals, but the resulting equations for the multi-compartment model are the same for a multiple-stage column.

The drops move along the z coordinate with velocity v_d, and their axial dispersion is modeled with an effective isotropic dispersion coefficient $D_{d,ef}$. The advective-diffusive flux F of drops of diameter d at any height in the column is given by:

$$F(t,z,d)=v_d(t,z,d,r_d)n(t,z,d)-\mathscr{D}_{d,ef}(t,z,r_d)\frac{\partial n}{\partial z} \tag{2}$$

where

$$r_d(t,z)=c_v\int_{d_{min}}^{d_{max}}d^3n(t,z,d)d(d) \tag{3}$$

is the dispersed phase fraction (holdup), being c_v a form factor that relates the drop diameter to its volume, $v(d)=c_vd^3$. For spherical drops, $c_v=\pi/6$.

The two-phase flow and mechanical agitation originate from the turbulent fluctuations in the continuous phase, which generate random drops movements. A dispersive flux is one way of modeling these drop movements. For staged extraction columns, mechanical agitation is the primary source of dispersion. In Eq. (2), we assumed the hypothesis that $\mathscr{D}_{d,ef}$ is independent from d.

In Eq. (1), the H term can be written as:

$$H=H_a+H_b \tag{4}$$

where H_a and H_b are the net rate of drop production by coalescence and breakage, respectively, that are assumed to be functions of the dispersed phase fraction (see Ramkrishna, 2000, for their general form). The breakage source terms are given by:

$$H_b=\int_d^{d_{max}}v(u)B(d|u)g(u,r_d)n(t,z,u)du-g(d,r_d)n(t,z,d) \tag{5}$$

where g, v and B are, respectively, the breakage frequency, the mean number of daughter drops and the daughter conditional probability distribution. We assumed that the latter depends only on the diameter ratio of daughter and mother drops. The coalescence source terms are given by:

$$\begin{aligned}H_a=&\ \tfrac{1}{2}\int_{d_{min}}^{d}\omega(u,s,r_d)n(t,z,u)n(t,z,s)\mathscr{J}du\\ &-\ n(t,z,d)\int_{d_{min}}^{u_{max}}\omega(u,d,r_d)n(t,z,u)du\end{aligned} \tag{6}$$

where $u_{max}=\left(d_{max}^3-d^3\right)^{1/3}$ and ω is the coalescence frequency that is assumed to be a function of the disperse phase fraction, and $\mathscr{J}$ is

the Jacobian of the transformation of the internal variable differential, $\mathscr{J}d(d) = ds$:

$$\mathscr{J} = \frac{d^2}{\left[d^3 - u^3\right]^{(2/3)}} \tag{7}$$

The number rate of drops entering the column can be modeled as a source at a given z_d position that is given by:

$$S(t,z,d) = \frac{Q_{d,in}(t)}{A}\frac{n_{in}(t,d)}{\bar{\upsilon}_{in}(t)}\delta(z - z_d) \tag{8}$$

where $Q_{d,in}(t)$ is the volumetric flow rate of the liquid that forms the drops fed to the column at point z_d and time t, A is the cross-section area of the column, and $n_{in}(t,d)$ is the normalized drop size distribution formed at the injection point, which satisfies:

$$\int_{d_{min}}^{d_{max}} n_{in}(t,d)d(d) = 1. \tag{9}$$

Thus, the mean drop volume at $z = z_d$ is given by:

$$\bar{\upsilon}_{in}(t) = \int_{d_{min}}^{d_{max}} \upsilon(d) n_{in}(t,d)d(d) \tag{10}$$

2.1.1. Boundary conditions

The Danckwerts boundary condition imposes the value of the advective-dispersive flux at the domain's boundaries. For the present model, the disperse phase is fed to the column at z_d, and the large ascending drops can leave the column at $z = h$, while the continuous phase carries the small descending drops that can leave the column at its bottom. We assumed that the dispersion flux is negligible at the top and bottom of the column, which is an adequate approximation for multi-stage columns with bottom and top sections with no mixing, which is the primary source of drop dispersion. Therefore, the imposed boundary conditions are:

$$\begin{aligned} z = 0, \quad F(t,0,d) = &\; v_d(t,0,d,r_d)n(t,0,d) - \mathscr{D}_{d,ef}(t,0,r_d)\tfrac{\partial n}{\partial z} \\ = &\; \min[v_d(t,0,d,r_d),0]n(t,0,d) \end{aligned} \tag{11}$$

$$\begin{aligned} z = h, \quad F(t,h,d) = &\; v_d(t,h,d,r_d)n(t,h,d) - \mathscr{D}_{d,ef}(t,h,r_d)\tfrac{\partial n}{\partial z} \\ = &\; \max[v_d(t,h,d,r_d),0]n(t,h,d) \end{aligned} \tag{12}$$

Considering the large ($v_d > 0$) and small ($v_d < 0$) drops, it is easy to prove that Eqs. (11) and (12) are equivalent to:

$$z = 0, \quad \max[v_d(t,0,d,r_d),0]n(t,0,d) - \mathscr{D}_{d,ef}(t,0,r_d)\frac{\partial n}{\partial z} = 0, \tag{13}$$

$$z = h, \quad \min[v_d(t,h,d,r_d),0]n(t,h,d) - \mathscr{D}_{d,ef}(t,h,r_d)\frac{\partial n}{\partial z} = 0, \tag{14}$$

which are the expressions given by Attarakih et al. (2004).

2.2. Drop and continuous phase velocities

The velocity of drops in a swarm significantly depends on the drop diameter and the volume fraction of the dispersed phase. The rising velocity v_d of a droplet of diameter d, is expressed as (Gayler et al., 1953):

$$v_d(d,r_d) = v_r(d,r_d) + v_c(r_d) \tag{15}$$

where v_c is the continuous phase velocity. The relative velocity of droplets with diameter d is often called the slip velocity. It is calculated from the single drop terminal velocity, v_t, considering the slowing factor and the swarm effect by the following expression:

$$v_r(d,r_d) = k_v v_t(1 - r_d)^{\kappa} \tag{16}$$

where $k_v \in (0,1]$ is the slowing factor and $(1 - r_d)^{\kappa}$ accounts for the swarm effect. The drop terminal velocity depends on the physical properties of both phases and droplet diameter (Garthe, 2006).

The steady-state solution of the mass balance equation for the continuous phase for a column operated in counter-current operation provides:

$$v_c(t,z) = \frac{1}{1 - r_d(t,z)}\left\{(1 - \mathscr{H}(z - z_c))\frac{Q_c}{A} + \mathscr{D}_{c,ef}(z)\frac{\partial r_d(t,z)}{\partial z}\right\} \tag{17}$$

where $\mathscr{D}_{c,ef}$ is the dispersion coefficient of the continuous phase that can be used to model backmixing.

2.3. Multi-compartment model for the extraction column

The one-dimensional model of an extraction column can have the external z coordinate domain partitioned to define compartments. These can be actual column stages in a multi-stage column or simply discretization subdomains in a continuous contact column. We consider a multi-compartment column with J sections operated in counter-current mode, where each section has a height h_j, as it is schematically represented in Fig. 1.

Its governing equation is given by Eq. (1), which can be integrated using the operator $\frac{1}{h_j}\int_{z_{j-1}}^{z_j}(\cdot)dz$to give:

$$\begin{aligned} \tfrac{\partial}{\partial t}\left[\tfrac{1}{h_j}\int_{z_{j-1}}^{z_j} n dz\right] + \tfrac{1}{h_j}(F_j - F_{j-1}) = &\; \tfrac{1}{h_j}\int_{z_{j-1}}^{z_j} S dz \\ + &\; \tfrac{1}{h_j}\int_{z_{j-1}}^{z_j} H dz, \quad j = 1,\ldots,J \end{aligned} \tag{18}$$

where

$$\begin{aligned} F_j(t,d) = F(t,z_j,d) = &\; v_d(t,z_j,d,r_d(t,z_j))n(t,z_j,d) \\ &-\mathscr{D}_{d,ef}(t,z_j,r_d(t,z_j))\left[\tfrac{\partial n(t,z,d)}{\partial z}\right]_{z=z_j} \end{aligned} \tag{19}$$

By defining the average of the generic ψ variable in the j compartment by:

$$\psi_j(t,d) = \frac{1}{h_j}\int_{z_{j-1}}^{z_j} \psi(t,z,d)dz, \tag{20}$$

we can write Eq. (18) as:

$$\frac{\partial n_j(t,d)}{\partial t} + \frac{1}{h_j}(F_j - F_{j-1}) = S_j + H_j, \quad J = 1,\ldots,J \tag{21}$$

Eq. (21) also represents the population balance model for each stage of a J-staged extraction column. In this case, we have to reinterpret the disperse-phase fluxes given by Eq. (19) as inter-stage fluxes. Then, we must use appropriate correlations (Hasseine et al., 2005) or CFD simulation data (Weber et al., 2020) for the specific type of staged column to calculate the absolute drop velocity and the drop dispersion coefficient.

The j control volume (compartment) is defined to be the column section in the $[z_{j-1}, z_j]$ interval. Therefore, all variables derived from the number size distribution are represented by its volumetric mean at this compartment, $n_j(t,d)$. For instance, the mean dispersed phase fraction in the j compartment is given by:

$$r_{dj}(t) = c_v \int_{d_{min}}^{d_{max}} d^3 n_j(t,d)d(d) \tag{22}$$

If any variable has a linear behavior within a compartment, then the value at its center is equal to the average, that is, $\psi(t, z_{j-1} + h_j/2, d) = \psi_j(t,d)$.

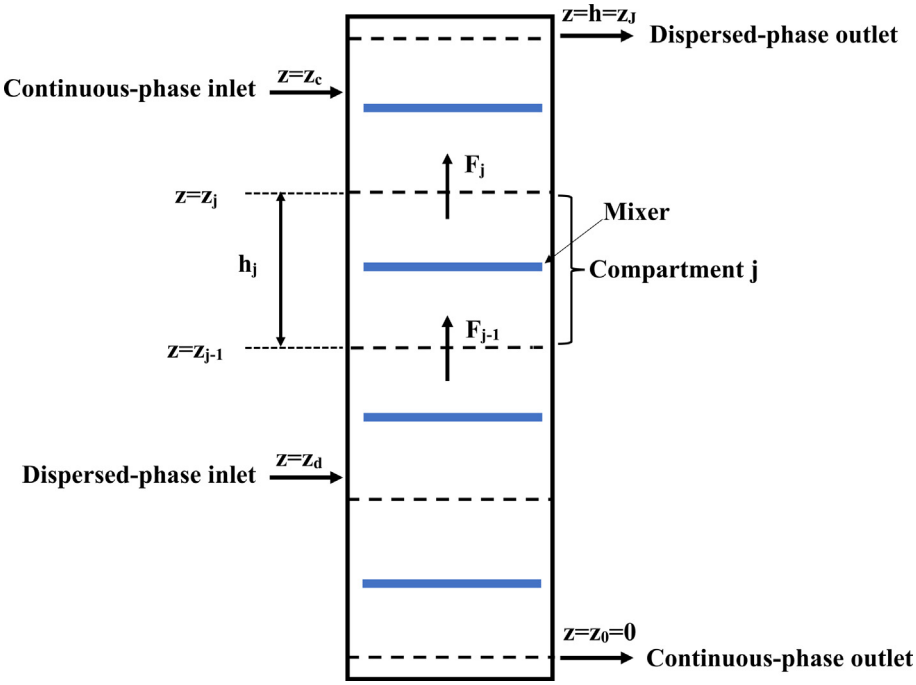

Fig. 1. Multi-compartment extraction column.

In Eq. (21), the source term S_j exists only for $j = j_d$, defined by $z_{j_d-1} < z_d < z_{j_d}$, where the drops are formed, which is given by:

$$S_j = S_{j_d}\delta_{jj_d}, \quad S_{j_d} = \frac{1}{h_{j_d}}\int_{z_{j_d-1}}^{z_{j_d}} S\,dz = \frac{1}{t_{h,j_d}}\frac{n_{in}(t,d)}{v_{in}} \tag{23}$$

where

$$t_{h,j_d} = \frac{h_{j_d}A}{Q_{d,in}} = \frac{V_{d_{j_d}}}{Q_{d,in}}, \quad V_{d_{j_d}} = h_{j_d}A \tag{24}$$

It should be noted that F_j must be computed at the boundary z_j between the j and $j+1$ compartments. Therefore, some approximations have to be made as the distribution n_j is a mean value for the j compartment.

As small drops can descend along the column dragged by the continuous phase, we must consider drop effluxes at z_0 and z_J. Moreover, every compartment boundary may have upward and downward drop fluxes. Therefore, we split the advective fluxes accordingly, and Eq. (19) becomes:

$$\begin{aligned} F(t,z_j,d) &= F_j(t,d) \\ &= F_j^+(t,d) + F_j^-(t,d) \\ &\quad - \mathscr{D}_{d,ef}\left(t,z_j,r_d(t,z_j)\right)\left[\frac{\partial n(t,z,d)}{\partial z}\right]_{z=z_j} \end{aligned} \tag{25}$$

We use a fully upwind approximation for the advective fluxes, that is,

$$\begin{aligned} F_j^-(t,d) &= \min(v_{d,j},0)n_{j+1}(t,d), \quad j=0,\ldots,J-1, \quad F_J^-(t,d)=0 \\ F_j^+(t,d) &= \max(v_{d,j},0)n_j(t,d), \quad j=1,\ldots,J, \quad F_0^+(t,d)=0 \end{aligned} \tag{26}$$

where $n(t,z_j,d) = n_j(t,d), v_{d,j}(t,d) = v_d(t,z_j,d,r_d(t,z_j))$ with $r_d(t,z_j) = r_j(t)$. Eq. (26) implies that there is no drop inlet at the column boundaries at z_0 and z_J.

Substituting Eqs. (26) into Eq. (25) and applying the boundary conditions given by Eqs. (11) and (12) under the assumption of no dispersive flux at the boundaries, we have:

$$F_0(t,d) = F_0^-(t,d) = \min(v_{d,0},0)n_1(t,d) \tag{27}$$

$$F_J(t,d) = F_J^+(t,d) = \max(v_{d,J},0)n_J(t,d) \tag{28}$$

Eqs. (27) and (28) are equivalent to the assumption of escape frequencies equal to $-v_{d,0}/h_0$ and $v_{d,J}/h_J$ for, respectively, the descending drops at the lowest compartment and the ascending drops at the highest compartment.

For the inter-compartment fluxes inside the column, we approximate the dispersive term by central differences:

$$\left[\frac{\partial n(t,z,d)}{\partial z}\right]_{z=z_j} = \frac{n_{j+1}(t,d)-n_j(t,d)}{\frac{h_{j+1}+h_j}{2}}, \tag{29}$$

The weighted harmonic mean is used to obtain the dispersion coefficient at the compartment boundaries:

$$\begin{aligned} \mathscr{D}_{d,ef,j+1/2}(t) &= \mathscr{D}_{d,ef}(t,z_j) \\ &= \left[\frac{1}{h_j+h_{j+1}}\left(\frac{h_j}{\mathscr{D}_{d,ef,j}(t)}+\frac{h_{j+1}}{\mathscr{D}_{d,ef,j+1}(t)}\right)\right]^{-1}, \end{aligned} \tag{30}$$

where $\mathscr{D}_{d,ef,j}(t)$ is the volumetric mean dispersion coefficient in compartment j. The harmonic mean used in Eq. (30) reduces to the correct limiting dispersive fluxes when $\mathscr{D}_{d,ef,i} \to 0$ or $\mathscr{D}_{d,ef,i} \to \infty$ for $i = j, j+1$ for transport processes in series. Using these approximations, we have

$$\begin{aligned} F_j(t,d) &= F_j^+(t,d) + F_j^-(t,d) - \mathscr{D}_{d,ef,j+1/2}(t) \\ &\quad \times \frac{2}{h_{j+1}+h_j}\left[n_{j+1}(t,d)-n_j(t,d)\right]. \end{aligned} \tag{31}$$

Thus, the multi-compartment model consists of the following ODE system for n_j:

$$\frac{\partial n_j}{\partial t} + \frac{1}{h_j}(F_j - F_{j-1}) = H_j + S_j, \quad j=1,\ldots,J \tag{32}$$

The breakage and coalescence source terms in compartment j can be written as:

$$H_j = H_{a,j} + H_{b,j} \tag{33}$$

Some definitions and approximations must be made to write these terms as functions of n_j. Lets assume that $n(t,z,d) = n_j(t,d)$for $z \in [z_{j-1}, z_j]$. Then, these distributions can be taken out of the z integral, and mean breakage and aggregation functions can be defined for each compartment. Assuming that $v(u)$ and $B(d|u)$do not depend on z, the breakage source term is given by:

$$H_{b,j} = \int_d^{d_{max}} v(u)B(d|u)g_j(u, r_{d,j})n_j(t,u)dudz - g_j(d, r_{d,j})n_j(t,d) \tag{34}$$

The coalescence source term is given by:

$$\begin{aligned} H_{a,j} = & \ \tfrac{1}{2}\int_{d_{min}}^{d} \omega_j(u,s,r_{d,j})n_j(t,u)n_j(t,s)\mathcal{J}du \\ - & \quad n_j(t,d)\int_{d_{min}}^{u_{max}} \omega_j(u,d,r_{d,j})n_j(t,u)du \end{aligned} \tag{35}$$

where

$$g_j\left(d, r_{d,j}(t)\right) = \frac{1}{h_j}\int_{z_{j-1}}^{z_j} g(d, r_d(t,z))dz \tag{36}$$

$$\omega_j\left(u, d, r_{d,j}(t)\right) = \frac{1}{h_j}\int_{z_{j-1}}^{z_j} \omega(u, d, r_d(t,z))dz \tag{37}$$

2.4. Model for the well-mixed vessel

The behavior of the dispersed phase in a continuous well-mixed vessel is a particular case of Eq. (32), where $J = j_d = 1$, $h_1 = h, t_{h,1} = t_h$ and, using Eq. (28), we have:

$$\frac{F_1}{h_1} = \frac{v_{d,1}}{h_1}n_1(t,d) = \frac{Q_{d,in}}{hA}n_1(t,d) = \frac{1}{t_h}n_1(t,d) \tag{38}$$

where in the last two expressions the drop escape frequency was assumed to be independent from its diameter and equal to the inverse of the mean residence time of the dispersed phase, t_h. Therefore, for the well-mixed vessel, the population balance equation can be written as (Ramkrishna, 2000):

$$\frac{\partial n(t,d)}{\partial t} = \frac{1}{t_h}\left[\frac{n_{in}(t,d)}{\bar{v}_{in}} - n(t,d)\right] + H_a(t,d) + H_b(t,d) \tag{39}$$

where the subscript 1 was dropped.

For a batch well-mixed vessel Eq. (39) takes the simple form:

$$\frac{\partial n(t,d)}{\partial t} = H_a(t,d) + H_b(t,d) \tag{40}$$

3. Generalized moment equations

Consider the generalized moment operator:

$$\langle \phi_k, (\cdot) \rangle = \int_{d_{min}}^{d_{max}} (\cdot)\phi_k(d)d(d), \tag{41}$$

where $\phi_k(d)$ is the Legendre polynomial of k degree defined into the shifted interval $[d_{min}, d_{max}]$, which have the following orthogonality property:

$$\langle \phi_k, \phi_j \rangle = \int_{d_{min}}^{d_{max}} \phi_k(d)\phi_j(d)d(d) = \delta_{kj}\langle \phi_k, \phi_k \rangle = \delta_{kj}\|\phi_k\|^2 \tag{42}$$

3.1. Moment equations for the multi-compartment model

The Legendre generalized moments of $n_j(t,d)$ can be computed from its definition, Eq. (20), and from Eq. (41) and they can be written as:

$$\mu_{j,k}^{(\phi)} = \langle \phi_k, n_j \rangle = \frac{1}{h_j}\int_{z_{j-1}}^{z_j} \langle \phi_k, n \rangle dz \tag{43}$$

Applying the moment operator, Eq. (41), to Eq. (32), we get:

$$\frac{\partial \mu_{j,k}^{(\phi)}}{\partial t} + \frac{1}{h_j}\left(\langle \phi_k, F_j \rangle - \langle \phi_k, F_{j-1} \rangle\right) = H_{j,k}^{(\phi)} + \frac{1}{t_{h,j_d}}\frac{\mu_{in_k}^{(\phi)}}{\bar{v}_{in}}\delta_{jj_d}, \quad j = 1, \ldots, J \tag{44}$$

where $\langle \phi_k, F_j \rangle$ are calculated using F_j from Eqs. (27), (28) and (31):

$$\begin{aligned} \langle \phi_k, F_0 \rangle = & \ \langle \phi_k, \min(v_{d,0}, 0)n_1 \rangle \\ \langle \phi_k, F_j \rangle = & \ \langle \phi_k, \max(v_{d,j}, 0)n_j \rangle + \langle \phi_k, \min(v_{d,j}, 0)n_{j+1} \rangle \\ & - \tfrac{2\mathscr{D}_{d,ef,j+1/2}}{h_{j+1}+h_j}\left[\mu_{j+1,k}^{(\phi)} - \mu_{j,k}^{(\phi)}\right], \quad j = 1, \ldots, J-1 \\ & \langle \phi_k, F_J \rangle = \langle \phi_k, \max(v_{d,J}, 0)n_J \rangle \end{aligned} \tag{45}$$

and

$$\mu_{in,k}^{(\phi)}(t) = \int_{d_{min}}^{d_{max}} n_{in}(t,d)\phi_k(d)d(d) \tag{46}$$

The moments of the breakage and coalescence terms in the j compartment are written as:

$$H_{j,k}^{(\phi)} = \langle \phi_k, H_j \rangle = \langle \phi_k, H_{a,j} \rangle + \langle \phi_k, H_{b,j} \rangle \tag{47}$$

Using the hypotheses described in Section 2.3, we can write the moments of the coalescence and breakage terms as:

$$\langle \phi_k, H_{a,j} \rangle = \tfrac{1}{2}\int_{d_{min}}^{d_{max}}\int_{d_{min}}^{d_{max}} \left[\phi_k\left(\left[s^3 + u^3\right]^{1/3}\right) - \phi_k(s) - \phi_k(u)\right] \omega_j(u,s)n_j(t,u)n_j(t,s)dsdu \tag{48}$$

$$\langle \phi_k, H_{b,j} \rangle = \int_{d_{min}}^{d_{max}} g_j(u)n_j(t,u)\left[v(u)\Pi_k^{(\phi)}(u) - \phi_k(u)\right]du \tag{49}$$

where

$$\Pi_k^{(\phi)}(u) = \int_{d_{min}}^{u} \phi_k(d)B(d|u)d(d) \tag{50}$$

3.2. Moment equations for the well-mixed vessel

This is a particular case of the model presented in the previous section. Thus, considering the same hypotheses described in Section 2.4, we can write the moments of the corresponding PBE by:

$$\frac{\partial \mu_k^{(\phi)}}{\partial t} = \frac{1}{t_h}\left[\frac{\mu_{in,k}^{(\phi)}}{\bar{v}_{in}} - \mu_k^{(\phi)}\right] + \langle \phi_k, H_a \rangle + \langle \phi_k, H_b \rangle \tag{51}$$

where

$$\mu_k^{(\phi)}(t) = \int_{d_{min}}^{d_{max}} n(t,d)\phi_k(d)d(d) \tag{52}$$

and $\langle \phi_k, H_a \rangle$ and $\langle \phi_k, H_b \rangle$ are those obtained from Eqs. 48,49 by dropping the j subscript.

4. The usage of a dimensionless internal variable

The internal variable d can be used to defined the dimensionless diameter x in the $[0,1]$ interval:.

$$x(d) = \frac{d - d_{min}}{d_{max} - d_{min}} \quad \Rightarrow \quad dx = \frac{d(d)}{d_{max} - d_{min}} \tag{53}$$

$$d(x) = d_{min} + x(d_{max} - d_{min}) \tag{54}$$

Considering the $n_j(t,d)$ distribution in the multi-compartment model, the transformed distribution $\tilde{n}_j(t,x)$ is given by:

$$n_j(t,d)d(d) = \tilde{n}_j(t,x)dx \quad \Rightarrow \quad \tilde{n}_j(t,x) = n_j(t,d)(d_{max} - d_{min}) \tag{55}$$

Defining $\varphi_k(x) = \phi_k(d(x))$, the following relation between the moment operators can be established:

$$\begin{aligned} \langle \varphi_k, (\cdot) \rangle = \int_0^1 (\cdot)\varphi_k(x)dx &= \frac{1}{d_{max} - d_{min}} \int_{d_{min}}^{d_{max}} (\cdot)\phi_k(d)d(d) \\ &= \frac{1}{d_{max} - d_{min}} \langle \phi_k, (\cdot) \rangle \end{aligned} \tag{56}$$

where $\langle (\cdot), (\cdot) \rangle$ indicates the inner product between two functions relatively to their internal variable, d or x. It should be pointed out that $\varphi_k(x)$ is just an expression for $\phi_k(d(x))$ and, therefore, both have the same dimensions, even though x is dimensionless.

Therefore, Eqs. (55) and (56) shows that:

$$\langle \varphi_k, \tilde{n}_j \rangle = \langle \phi_k, n_j \rangle \tag{57}$$

Similarly

$$\tilde{n}_{in}(t,x) = (d_{max} - d_{min})n_{in}(t,d) \quad \Rightarrow \quad \langle \varphi_k, \tilde{n}_{in} \rangle = \langle \phi_k, n_{in} \rangle \tag{58}$$

If we define:

$$\widetilde{F}_j(t,x) = (d_{max} - d_{min})F_j(t,d), \tag{59}$$

$$\widetilde{H}_{a,j}(t,x) = (d_{max} - d_{min})H_{a,j}(t,d) \tag{60}$$

$$\widetilde{H}_{b,j}(t,x) = (d_{max} - d_{min})H_{b,j}(t,d) \tag{61}$$

then

$$\left\langle \varphi_k, \widetilde{F}_j \right\rangle = \langle \phi_k, F_j \rangle \tag{62}$$

$$\left\langle \varphi_k, \widetilde{H}_{a,j} \right\rangle = \langle \phi_k, H_{a,j} \rangle \tag{63}$$

$$\left\langle \varphi_k, \widetilde{H}_{b,j} \right\rangle = \langle \phi_k, H_{b,j} \rangle \tag{64}$$

4.1. Moment equations of the multi-compartment model

Considering Eqs. (57), (58), (62), (63) and (64), the moment equations of the multi-compartment model, given by Eq. (44), can be written as:

$$\begin{aligned} &\frac{\partial \mu_{j,k}^{(\varphi)}}{\partial t} + \frac{1}{h_j}\left(\left\langle \varphi_k, \widetilde{F}_j \right\rangle - \left\langle \varphi_k, \widetilde{F}_{j-1} \right\rangle\right) \\ &\quad = \left\langle \varphi_k, \widetilde{H}_j \right\rangle + \frac{1}{t_{h,j_d}} \frac{\mu_{in,k}^{(\varphi)}}{\bar{v}_{in}} \delta_{j,j_d}, \quad j = 1, \ldots, J \end{aligned} \tag{65}$$

where

$$\begin{aligned} &\left\langle \varphi_k, \widetilde{F}_0 \right\rangle = \langle \varphi_k, \min(v_{d,0}, 0)\tilde{n}_1 \rangle, \\ &\left\langle \varphi_k, \widetilde{F}_j \right\rangle = \langle \varphi_k, \max(v_{d,j}, 0)\tilde{n}_j \rangle + \langle \varphi_k, \min(v_{d,j}, 0)\tilde{n}_{j+1} \rangle \\ &\quad - \frac{2\mathscr{D}_{d,ef\,j+1/2}}{h_{j+1} + h_j}\left[\mu_{j+1,k}^{(\varphi)} - \mu_{j,k}^{(\varphi)}\right], \quad j = 1, \ldots, J-1, \\ &\left\langle \varphi_k, \widetilde{F}_J \right\rangle = \langle \varphi_k, \max(v_{d,J}, 0)\tilde{n}_J \rangle, \end{aligned} \tag{66}$$

and

$$\begin{aligned} \left\langle \varphi_k, \widetilde{H}_{a,j} \right\rangle = \tfrac{1}{2} \int_0^1 \int_0^1 &[\varphi_k(q(x,y)) - \varphi_k(y) - \varphi_k(x)] \\ &\tilde{\omega}_j(x,y)\tilde{n}_j(t,x)\tilde{n}_j(t,y)dydx \end{aligned} \tag{67}$$

where $q(x,y)$ is the value of the dimensionless diameter of the daughter drop formed by the coalescence of drops with dimensionless diameters $x(d)$ and $y(u)$ and $\tilde{\omega}_j(x(d), y(u)) = \omega_j(d,u)$. The breakage term becomes:

$$\left\langle \varphi_k, \widetilde{H}_{b,j} \right\rangle = \int_0^1 \tilde{g}_j(x)\tilde{n}_j(t,x)\left[\tilde{\nu}(x)\tilde{\Pi}_k^{(\varphi)}(x) - \varphi_k(x)\right]dx \tag{68}$$

where $\tilde{g}_j(x(d)) = g_j(d)$ and

$$\begin{aligned} \Pi_k^{(\phi)}(u(x)) &= \int_{d_{min}}^{u(x)} \phi_k(d(y))B(d(y)|u(x))d(d) \\ &= \int_0^x \varphi_k(y)\widetilde{B}(y|x)dy = \tilde{\Pi}_k^{(\varphi)}(x). \end{aligned} \tag{69}$$

4.2. Moment equations for the continuous well-mixed vessel

As before, this is a special case of the multicompartment model with just one compartment. Therefore, the moment equations in the dimensionless internal variable come from Eq. (65) with $J = 1$. Using the same approximations described in Section 2.4, we have:

$$\frac{\partial \mu_k^{(\varphi)}}{\partial t} = \frac{1}{t_h}\left[\frac{\mu_{k,in}^{(\varphi)}}{\bar{v}_{in}} - \mu_k^{(\varphi)}\right] + \left\langle \varphi_k, \widetilde{H}_a \right\rangle + \left\langle \varphi_k, \widetilde{H}_b \right\rangle \tag{70}$$

and $\left\langle \psi_k, \widetilde{H}_a \right\rangle$ and $\left\langle \psi_k, \widetilde{H}_b \right\rangle$ are those obtained from Eqs. (67)–(69) by dropping the j subscript.

5. Application of the DuQMoGeM to the models

The DuQMoGeM employs two quadrature rules (Lage, 2011). The first one is the N_q-point Gauss-Christoffel quadrature based on the $2N_q$ moments of the particle number distribution function. It is used to discretize the distribution. The second quadrature rule is a M-point Gaussian quadrature based on an orthogonal polynomial family that is used to calculate the integrals related to the internal variable with controlled accuracy. It is strongly recommended that $M > 2N_q$ to guarantee the correct integration of the expansion coefficients of Eq. (74) when it is substituted into Eq. (75).

For continuous distributions, the $2N_q$ generalized moments of the distribution are directly related to a $(2N_q - 1)$-order series expansion using the orthogonal polynomial family employed to generate the second quadrature. Here, all models were solved using the dimensionless internal variable x, and, therefore, we employed the Legendre polynomials shifted to the $[0,1]$ interval, $\varphi_k(x)$.

5.1. The Gauss-Legendre quadrature

The Gauss-Legendre quadrature in the $[0,1]$ interval approximates the following integral of a generic function G:

$$\int_0^1 G(x)dx \approx \sum_{i=1}^{M} w_i G(\xi_i) \tag{71}$$

where w_i are the weights and ξ_i are the abscissas of the quadrature rule. As it gives the correct value of the integral when G is a polynomial whose order is equal to or less than $2M - 1$, the result for $G(x) = 1$ gives that:

$$\sum_{i=1}^{M} w_i = 1 \tag{72}$$

If an integral in the incomplete interval $[0,x]$ is necessary, one just has to define $Y = y/x$:

$$\int_0^x G(y)dy = x\int_0^1 G(xY)dY = x\sum_{i=1}^{M} w_i G(\xi_i x) = \sum_{i=1}^{M} w_{x,i} G(\xi_{x,i}) \tag{73}$$

where $w_{x,i} = xw_i$ and $\xi_{x,i} = x\xi_i$.

5.2. DuQMoGeM solution for the multi-compartment extraction column

For this case, the mean distribution function at each compartment, $\tilde{n}_j(t,x)$, is approximated by the polynomial series of $2N_q - 1$ order:

$$\tilde{n}_j(t,x) = \sum_{i=0}^{2N_q-1} c_{j,i}(t)\varphi_i(x) \tag{74}$$

where

$$c_{j,i}(t) = \frac{\langle \tilde{n}_j, \varphi_i\rangle}{\langle \varphi_i, \varphi_i\rangle} = \frac{1}{\|\varphi_i\|^2}\int_0^1 \tilde{n}_j(t,x)\varphi_i(x)dx = \frac{\mu_{j,i}^{(\varphi)}(t)}{\|\varphi_i\|^2},$$
$$i = 0,1,\ldots,2N_q-1 \tag{75}$$

Although Eq. (74) provides an approximate representation of the drop number distribution, it must be emphasized that the DuQMoGeM is a moment method, and its solution consists of the generalized moments, $\mu_{j,i}^{(\varphi)}$.

Substitution (74) and (75) in (65) gives:

$$\begin{aligned}\|\varphi_k\|^2 \frac{\partial c_{j,k}(t)}{\partial t} &= \frac{1}{h_j}\left(\left\langle \varphi_k, \widetilde{F}_{j-1}\right\rangle - \left\langle \varphi_k, \widetilde{F}_j\right\rangle\right) + \frac{1}{t_{h_{j_d}}}\frac{\mu_{in,k}^{(\varphi)}}{\bar{v}_{in}}\delta_{jj_d} \\ &+ \sum_{i=0}^{2N_q-1}\sum_{l=0}^{2N_q-1} \mathscr{A}_{jkli}c_{j,l}c_{j,i} + \sum_{i=0}^{2N_q-1}\mathscr{L}_{jki}c_{ji}, \quad j = 1,\ldots,J\end{aligned} \tag{76}$$

where, from Eq. (66):

$$\begin{aligned}\left\langle \varphi_k, \widetilde{F}_0\right\rangle &= \left\langle \varphi_k, \min(v_{d,0},0)\tilde{n}_1\right\rangle \\ \left\langle \varphi_k, \widetilde{F}_j\right\rangle &= \left\langle \varphi_k, \max(v_{d,j},0)\tilde{n}_j\right\rangle + \left\langle \varphi_k, \min(v_{d,j},0)\tilde{n}_{j+1}\right\rangle \\ &- \frac{2\mathscr{D}_{d,ef,j+1/2}}{h_{j+1}+h_j}\|\varphi_k\|^2\left[c_{j+1,k} - c_{j,k}\right],\ j = 1,\ldots,J-1 \\ \left\langle \varphi_k, \widetilde{F}_J\right\rangle &= \left\langle \varphi_k, \min(v_{d,J},0)\tilde{n}_J\right\rangle\end{aligned} \tag{77}$$

The advective terms in Eq. (77) can be approximated by:

$$\left\langle \varphi_k, \max(v_{d,j},0)\tilde{n}_j\right\rangle = \sum_{i=0}^{2N_q-1} c_{j,i}\mathscr{V}_{jki}^{+}, \tag{78}$$

$$\left\langle \varphi_k, \min(v_{d,j},0)\tilde{n}_{j+1}\right\rangle = \sum_{i=0}^{2N_q-1} c_{j+1,i}\mathscr{V}_{jki}^{-} \tag{79}$$

where

$$\mathscr{V}_{jki}^{+} = \left\langle \varphi_k, \max(v_{d,j},0)\varphi_i\right\rangle = \int_0^1 \varphi_k(x)\varphi_i(x)\max\left[v_{dj}(t,d(x)),0\right]dx, \tag{80}$$

$$\mathscr{V}_{jki}^{-} = \left\langle \varphi_k, \min(v_{d,j},0)\varphi_i\right\rangle = \int_0^1 \varphi_k(x)\varphi_i(x)\min\left[v_{dj}(t,d(x)),0\right]dx. \tag{81}$$

Using Eqs. (67) and (68), the breakage and coalescence terms can be written as:

$$\begin{aligned}\mathscr{L}_{jki} &= \left\langle \tilde{g}_j\left[\tilde{\nu}\tilde{\Pi}_k^{(\varphi)} - \varphi_k\right], \varphi_i\right\rangle \\ &= \int_0^1 \tilde{g}_j(x)\varphi_i(x)\left[\tilde{\nu}(x)\tilde{\Pi}_k^{(\varphi)}(x) - \varphi_k(x)\right]dx,\end{aligned} \tag{82}$$

$$\begin{aligned}\mathscr{A}_{jkli} &= \left\langle\left\langle[\varphi_k(q(x,y)) - \varphi_k(y) - \varphi_k(x)]\tilde{\omega}_j(x,y), \varphi_l(y)\right\rangle, \varphi_i(x)\right\rangle \\ &= \tfrac{1}{2}\int_0^1\int_0^1 [\varphi_k(q(x,y)) - \varphi_k(y) - \varphi_k(x)]\tilde{\omega}_j(x,y)\varphi_i(x)\varphi_l(y)dydx\end{aligned} \tag{83}$$

Applying the Gauss-Legendre quadrature given by Eq. (71) to the above integrals, we have:

$$\mathscr{V}_{jki}^{+} = \sum_{r=1}^{M} w_r\varphi_k(\xi_r)\varphi_i(\xi_r)v_{dj}(t,d(\xi_r)), \quad v_{dj}(t,d(\xi_r)) \geqslant 0 \tag{84}$$

$$\mathscr{V}_{jki}^{-} = \sum_{r=1}^{M} w_r\varphi_k(\xi_r)\varphi_i(\xi_r)v_{dj}(t,d(\xi_r)), \quad v_{dj}(t,d(\xi_r)) < 0 \tag{85}$$

$$\mathscr{L}_{jki} = \sum_{r=1}^{M} w_r\tilde{g}_j(\xi_r)\varphi_i(\xi_r)\left[\tilde{\nu}(\xi_r)\tilde{\Pi}_k^{(\varphi)}(\xi_r) - \varphi_k(\xi_r)\right], \tag{86}$$

$$\mathscr{A}_{jkli} = \frac{1}{2}\sum_{r=1}^{M}\sum_{p=1}^{M} w_r w_p\left[\varphi_k\left[q(\xi_p,\xi_r)\right] - \varphi_k(\xi_p) - \varphi_k(\xi_r)\right]\tilde{\omega}_j(\xi_r,\xi_p)\varphi_i(\xi_r)\varphi_l(\xi_p). \tag{87}$$

For the moments of the daughter distribution function, defined in eq. (69), the quadrature rule in the incomplete interval given by Eq. (73) gives:

$$\tilde{\Pi}_k^{(\varphi)}(\xi_r) = \xi_r\sum_{m=1}^{M} w_m\varphi_k(\xi_r\xi_m)\widetilde{B}(\xi_r\xi_m|\xi_r). \tag{88}$$

5.3. DuQMoGeM solution for the well-mixed vessel

This solution can be obtained by applying the multi-compartment model with $J = j_d = 1$. Using Eq. (76) and the same simplifications described in Section 2.4, we have:

$$\|\varphi_k\|^2\frac{\partial c_k(t)}{\partial t} = \frac{\mu_{in,k}^{(\varphi)}}{t_h\bar{v}_{in}} - \frac{1}{t_h}\|\varphi_k\|^2 c_k(t) + \sum_{i=0}^{2N_q-1}\sum_{l=0}^{2N_q-1}\mathscr{A}_{kli}c_l c_i + \sum_{i=0}^{2N_q-1}\mathscr{L}_{ki}c_i \tag{89}$$

where

$$\tilde{n}(t,x) = \sum_{i=0}^{2N_q-1} c_i(t)\varphi_i(x), \quad c_i(t) = \frac{\mu_i^{(\varphi)}(t)}{\|\varphi_i\|^2} \tag{90}$$

where $\mathscr{L}_{ki}$ and $\mathscr{A}_{kli}$ are calculated as given by Eqs. (86) and (87) after dropping the j subscript.

6. Numerical procedure

The DuQMoGeM equations for the J-compartment model form a system of $(2N_qJ)$ ordinary differential equations that were coded in a FORTRAN program that used the DASSL package (Petzold, 1982) for time integration with controlled local accuracy. This integration was carried out in double precision with the $c_{j,i}$ coefficients as the dependent variables. These are then used to compute the generalized moments and the series approximation of the drop number distributions in all compartments. In all cases, the DASSL routine employed values for the absolute and relative tolerances equal to 10^{-11}.

The ORTHPOL package (Gautschi, 1994) routines were used to compute the polynomial recursion coefficients and quadrature rules. The routine *drecur* with *ipoly* = 2 gives the first M pairs of recursion coefficients for the three-term recurrence relation for

the Legendre polynomials shifted to the $[0,1]$ interval that are fed to the *dgauss* routine to compute the Gauss-Legendre quadrature rule for this interval, that is, its abscissas, ξ_i, and weights, $w_i, i = 1,\ldots,M$.

If a discretization of the distribution is desired, the $2N_q$ first Legendre-generalized moments of the distribution, $\mu_{j,i}^{(\varphi)}, i = 0, 1,\ldots,2N_q - 1$ can be fed to the *dcheb* routine to provide the first N_q pairs of recursion coefficients for the three-term recurrence relation for the polynomials that are orthogonal in respect to the measure given by the distribution. Then, these recursion coefficients can be used as input to the *dgauss* routine to compute the N_q-point Gauss-Christoffel quadrature rule.

7. Results

In order to present the results clearly, we divided this section into four subsections, each one devoted to presenting results for one of the following systems: batch extraction vessel, continuous flow extraction vessel, extraction columns, all of them solved for problems with known analytical solutions, and an extraction column with available experimental data.

The batch extraction vessel section shows DuQMoGeM results for problems with pure breakage, pure coalescence, and simultaneous breakage and coalescence. The continuous flow extraction vessel section presents DuQMoGeM results for pure breakage and pure coalescence problems. The convergence of the lowest order moments regarding the number of points in the first quadrature, N_q, was studied for these well-mixed vessel solutions. Analytical solutions exist for extraction column problems with no drop dispersion and constant drop ascension velocity assumptions. The extraction column section presents DuQMoGeM solutions for three such cases: pure breakage, pure coalescence, and simultaneous breakage and coalescence. The convergence of results regarding the number of compartments was analyzed. In the final section, we compared the DuQMoGeM prediction of the hold up of the dispersed phase with available experimental data for a Kühni column operated with the toluene-water system. We modeled the Kühni column, including drop advective and dispersive transport, breakage, and coalescence.

In fact, the verification problems were solved analytically in the semi-finite range, $[0,\infty)$, while the DuQMoGeM solutions were solved for the range $[d_{min}, d_{max}]$. However, we guaranteed that the supports of the number density distributions given by the analytical solutions were always within the $[d_{min}, d_{max}]$ range for the analyzed time interval. We also assumed spherical droplets.

7.1. Batch extraction vessel

For the batch extraction vessel, we applied the DuQMoGeM solution to Eq. 40, for which three cases with available analytical solutions were considered: a pure breakage, a pure coalescence, and a simultaneous breakage and coalescence problems. In fact, the last two cases were solved previously by Lage (2011) using the DuQMoGeM, but employing the particle volume in the semi-infinite domain as the internal variable. In this section, all variables are considered dimensionless.

7.1.1. Pure coalescence in finite domain, $d \in [0, 6.0]$

When the drops undergo coalescence with a constant kernel ($\omega = 1$ for this case) and with an exponential initial distribution given by

$$n(0,d) = \upsilon'(d)\exp[-\upsilon(d)], \tag{91}$$

the analytical solution was reported by Gelbard and Seinfeld (1978) as:

$$n(t,d) = \frac{4\upsilon'(d)}{(\omega t+2)^2}\exp\left(-\frac{2\upsilon(d)}{\omega t+2}\right), \tag{92}$$

where $\upsilon(d) = c_\upsilon d^3$ and $\upsilon'(d) = d\upsilon/d(d) = 3c_\upsilon d^2$.

Under these conditions, we investigated the effect of the number of the Gauss-Christoffel quadrature points on the absolute errors of the first four moments. Fig. 2 shows that the absolute error decreases by increasing the number of the Gauss-Christoffel quadrature N_q, being the best results generated for $N_q = 6$. This figure shows that the DuQMoGeM accuracy for the zeroth-order moment is better than for the first and second-order moments. The third-order moment has an error close to the machine's accuracy because it is unchanged throughout the evolution of the distribution as the breakage phenomenon conserves the total volume (mass) of the particles.

Fig. 3 presents the analytical solution and the numerical distribution function computed with $N_q = 6$ and $M = 12$ for this case for three instants, showing perfect agreement between the analytical distributions and their DuQMoGeM approximations.

7.1.2. Pure breakage in finite domain, $d \in [0,2]$

In this case, a normal Gaussian distribution with mean $m = 0.9$ and standard deviation $\alpha = 0.8$ was used as the initial condition as given by:

$$n(0,d) = \frac{\upsilon'(d)}{\sqrt{2\pi}\alpha}\exp\left[-\frac{(\upsilon(d)-m)^2}{\Lambda}\right] \tag{93}$$

where $\Lambda = 2\alpha^2$. For a daughter drop distribution given by $B(d|u) = 6d^2/u^3$and a breakage frequency linear in drop volume, $g(d) = \upsilon(d)$, Hasseine et al. (2020) provided the exact solution that can be writen as:

$$n(t,d) = \upsilon'(d)\frac{2\chi + \Lambda t^2\chi + \sqrt{\Lambda}\sqrt{\pi}\Phi(2t + mt^2 - t^2\upsilon(d))}{2\sqrt{2\pi}\alpha} \times \exp[-t\upsilon(d)] \tag{94}$$

where

$$\chi = \exp\left[-\frac{(\upsilon(d)-m)^2}{2\alpha^2}\right] \quad \text{and} \quad \Phi = 1 + \operatorname{erf}\left[\frac{m-\upsilon(d)}{\sqrt{\Lambda}}\right] \tag{95}$$

Fig. 4(a) shows a comparison between the analytical moments of $n(t,d)$ with those obtained from DuQMoGeM solution for $N_q = 4$ and $M = 8$, which show excellent agreement. The results show that the total volume of the droplets, μ_3, remains constant. The moments of the order lower than three increase, whereas μ_4 and μ_5 decrease. Fig. 4(b) shows the good agreement between the exact and the numerical distributions obtained from DuQMoGeM at different times using $N_q = 6$ and $M = 12$.

7.1.3. Simultaneous breakage and coalescence in finite domain, $d \in [0, 2.8]$

We considered here the combined coalescence and breakage problem with $\omega(v,u) = 1, g(d) = g_0\upsilon(d), g_0 = 2$, and $B(d/u) = 6d^2/u^3$. For the initial condition described by Eq. (91), McCoy and Madras (2003) gave the following analytical solution:

$$n(t,d) = \upsilon'(d)[\Phi(t)]^2\exp[-\Phi(t)\upsilon(d)] \tag{96}$$

where

$$\Phi(t) = \Phi(\infty)\frac{1+\Phi(\infty)\tanh(\Phi(\infty)t/2)}{\Phi(\infty)+\tanh(\Phi(\infty)t/2)}, \quad \Phi(\infty) = \sqrt{2g_0} \tag{97}$$

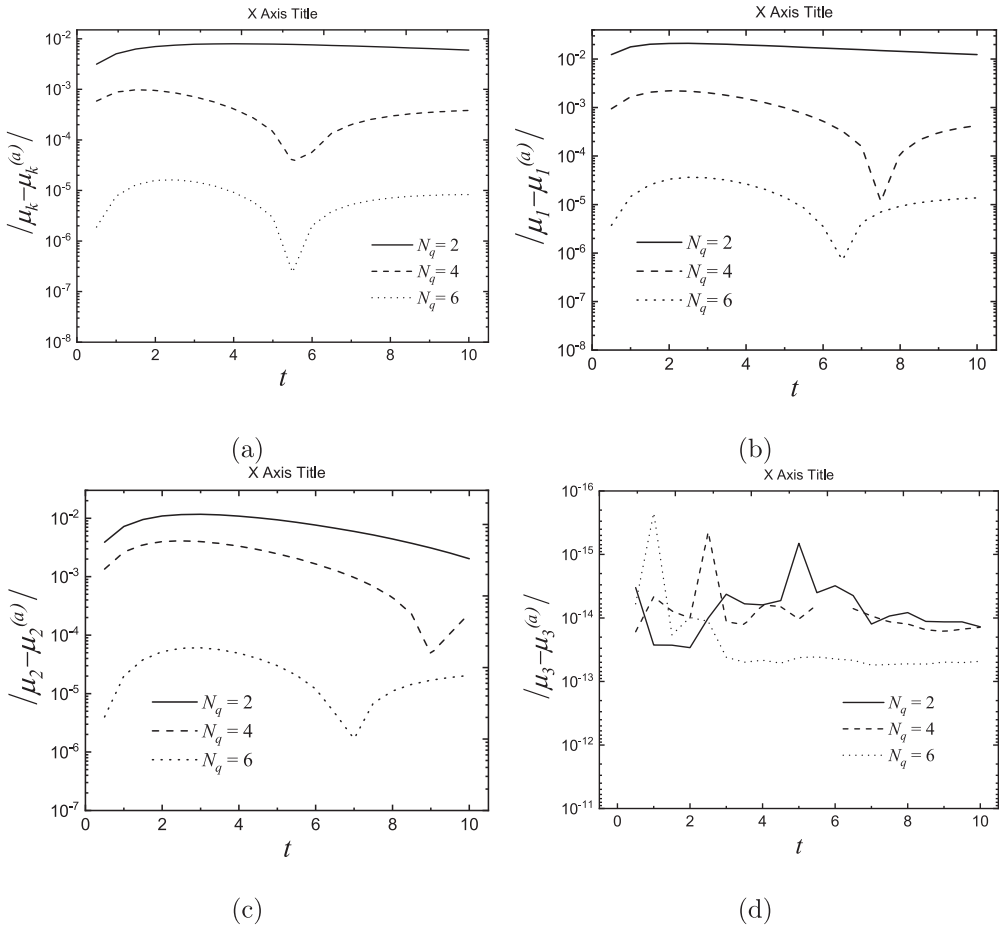

Fig. 2. Pure coalescence problem in a batch extraction vessel: absolute errors for the first four regular moments for the DuQMoGeM solutions with $N_q = 2, 4$ and 6 using the same number of Gauss-Legendre quadrature points, $M = 12$.

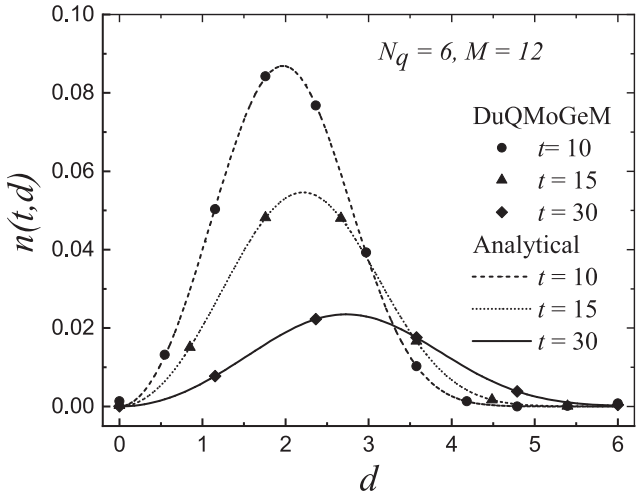

Fig. 3. Pure coalescence problem in a batch extraction vessel: comparison of the analytical and numerical distributions.

Fig. 5 shows the series approximation of the number density distribution for the numerical solution with $N_q = 6$ and $M = 12$ at different values of t, showing a good agreement with the analytical solution.

7.2. Continuous flow extraction vessel

The performance of the DuQMoGeM to solve the PBE in the continuous flow well-mixed extraction vessel is tested for two different cases: one with droplet coalescence and other with droplet breakage. In this section, all variables are considered dimensionless.

7.2.1. Pure breakage in finite domain, $d \in [0, 1.9]$

This case is similar to first case of pure breakage but in a continuous flow extraction vessel with $t_h = 10^3$. The inlet drop number distribution, $n_{in}(t,d)$, is the normal Gaussian distribution with mean $m = 0.9$ and standard deviation $\alpha = 0.8$ given by Eq. (93). Initially, there is no drop in the reactor, and, thus, $n(0,d) = 0$. This problem comes from Hasseine et al. (2020) and its analytical solution is:

$$\begin{aligned} n(t,d) = \tfrac{\upsilon'(d)a}{2\sqrt{2\pi}\alpha\beta(t,d)[a+\upsilon(d)]^3}\Big\{ & 2[-1+\beta(t,d)][\upsilon(d)]^2\chi \\ & +\Lambda\Big[-2+2\beta(t,d)-2t\upsilon(d)-t^2[\upsilon(d)]^2\Big]\chi \\ & +\sqrt{\Lambda}\sqrt{\pi}\Big[t^2[\upsilon(d)]^3+m\Big(-2+2\beta(t,d)-2t\upsilon(d)-t^2[\upsilon(d)]^2\Big)\Big]\Phi \\ & +a^2\Big[(-2+2\beta(t,d)-\Lambda t^2)\chi+\sqrt{\Lambda}\sqrt{\pi}t(-2-mt+t\upsilon(d))\Phi\Big] \\ & -2a[-2(-1+\beta(t,d))\upsilon(d)\chi+\Lambda t(1+t\upsilon(d))\chi \\ & -\sqrt{\Lambda}\sqrt{\pi}\Big\{-1+\beta(t,d)-t\upsilon(d)+t^2(\upsilon(d))^2-mt[1+t\upsilon(d)]\Big\}\Phi\Big]\Big\} \end{aligned} \tag{98}$$

where $a = t_h^{-1}$ and $\beta(t,d) = \exp\{t[a+\upsilon(d)]\}$.

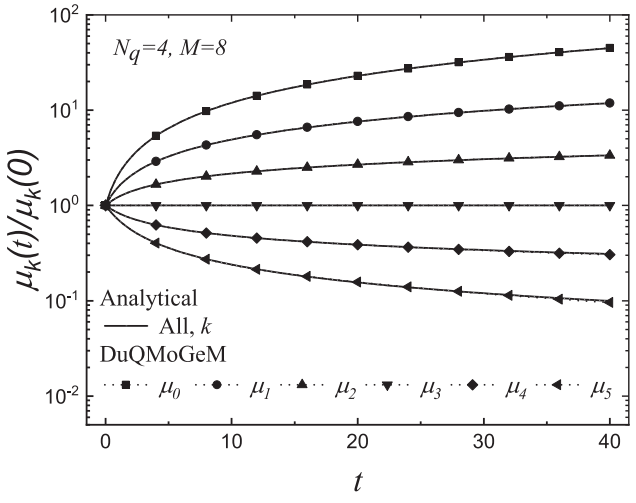

(a)

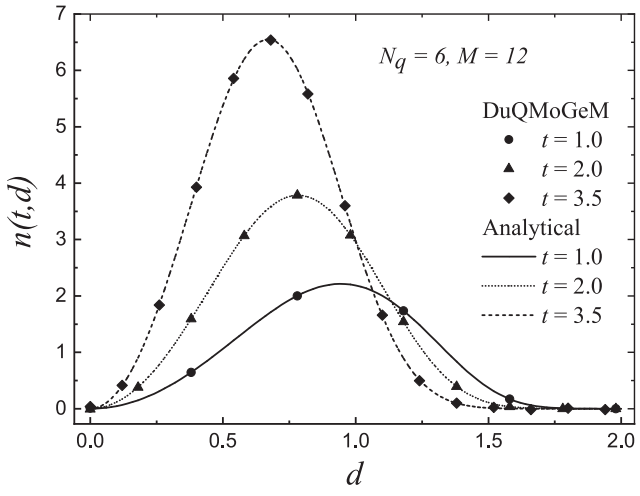

(b)

Fig. 4. Pure breakage problem in a batch extraction vessel: comparison of the analytical and numerical results.

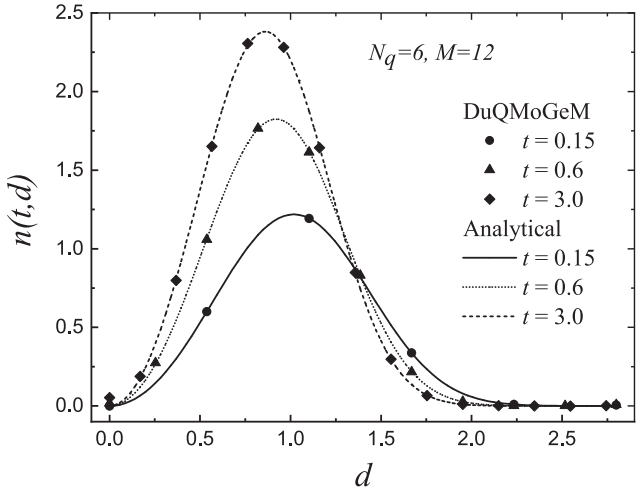

Fig. 5. Simultaneous breakage and coalescence problem in batch extraction vessel: comparison of the analytical and numerical distributions.

Fig. 6(a) shows the regular moments obtained from DuQMoGeM solution with $N_q = 6$ and $M = 12$ together with those computed from the exact solution. The results demonstrate that all moments increase with time. The numerical and analytical results for all moments are in good agreement. Fig. 6(b) shows the exact and the numerical distribution obtained from DuQMoGeM at different values of t. The agreement between the numerical and analytical distributions is excellent.

7.2.2. Pure coalescence in finite domain, $d \in [0, 4.6]$

The population balance equation in a continuous flow well-mixed extraction vessel was solved dynamically using the DuQMoGeM for a pure coalescence problem with a constant aggregation kernel ($\omega = 1$). The initial condition is zero, $n(0,d) = 0$, while the drop number distribution at the inlet, $n_{in}(t,d)$, has the same distribution given by Eq. (91). Hounslow (1990) solved this problem at the steady state and found the following exact solution:

$$n(\infty,d) = \frac{\upsilon'(d)}{\sqrt{1+2t_h}} \exp\left[-\frac{(1+t_h)\upsilon(d)}{1+2t_h}\right]\left[I_0\left(\frac{-t_h\upsilon(d)}{1+2t_h}\right) + I_1\left(\frac{-t_h\upsilon(d)}{1+2t_h}\right)\right] \tag{99}$$

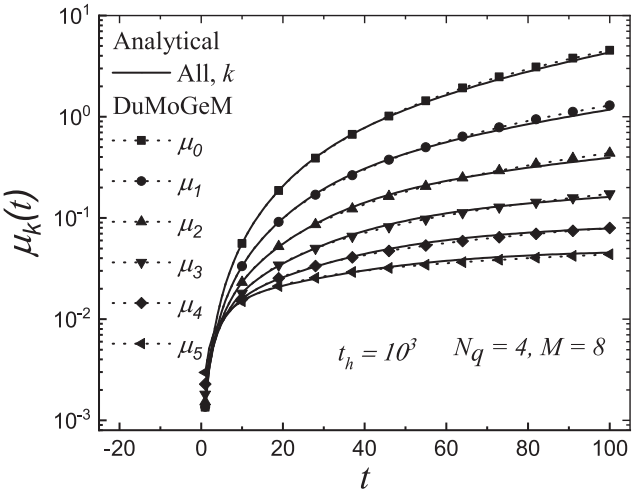

(a)

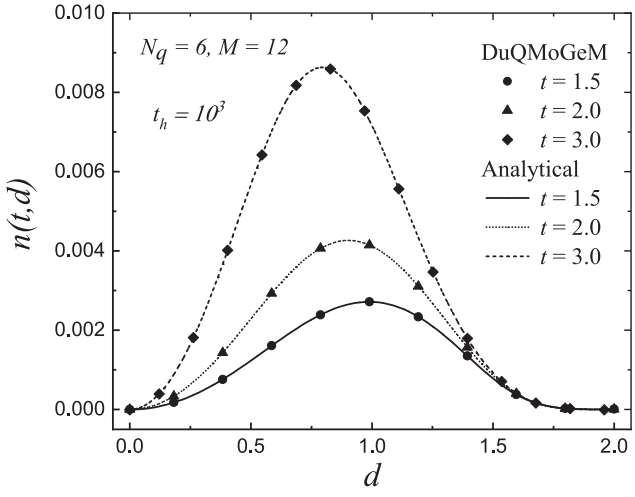

(b)

Fig. 6. Pure breakage problem in a continuous flow extraction vessel: comparison of the analytical and numerical results.

where I_0 and I_1 are the modified Bessel functions of the first kind and zeroth and first orders, respectively.

The simulation was implemented with $N_q = 3$ and $M = 6$ and $t_h = 10$. In order to verify the DuQMoGeM results, for different values of t, the distributions obtained by the DuQMoGeM are presented with the exact solution described by the above equation in Fig. 7(a). The numerical distributions for $t \geqslant 30$ conform with its steady-state analytical solution. The dynamically predicted and the analytical steady-state moments are presented in Fig. 7 (b). As expected for a first-order system, the process reaches the steady state for $t/t_h \approx 4$.

7.3. Hydrodynamics simulation of extraction columns

The DuQMoGeM solution of the multi-compartment model was obtained for three test cases: pure breakage, pure coalescence and breakage with coalescence. We assumed pure drop advection with a constant velocity because the analytical solutions are known for these three cases under this assumption, being provided by Attarakih et al. (2004) and Hasseine et al. (2018). In this section, all variables are considered dimensionless.

All simulations assumed no drops initially present in the column, $Q_d/A = 1$, $v_d = 1$, and inlet drop number distribution given by:

$$N_0 n_{in}(t,d) = \upsilon'(d)\frac{N_0}{\bar{v}_{in}}\exp\left[-\frac{\upsilon(d)}{\bar{v}_{in}}\right] \tag{100}$$

where the drop number density, N_0, and the mean volume, $\bar{v}_{in}$, were chosen to be 0.05 and 1, respectively. For each case, the employed breakage and coalescence functions are reported in Table 1. Solutions are presented along the dimensionless vertical coordinate, $\zeta = z/h$ and the injection point of the disperse phase is located at $\zeta = 0.1$. For all cases, the simulation results were obtained assuming an uniform compartment height.

7.3.1. Case 1: pure breakage, $d \in [0, 2.5]$

The analytical solution is described as follows:

$$n(t,z,d) = \upsilon'(d)\frac{N_0}{\bar{v}_{in}} \times \exp\left[-(1+g_0\Delta z)\frac{\upsilon(d)}{\bar{v}_{in}}\right](1+g_0\Delta z)^2\mathscr{H}\left[t-\frac{\Delta z}{v_d}\right] \tag{101}$$

where $\Delta z = z - z_d$ and $\mathscr{H}$ is the Heaviside step function.

7.3.2. Case 2: pure coalescence, $d \in [0, 3.8]$

The exact solution for this case is written as:

$$n(t,z,d) = \upsilon'(d)\frac{N_0}{\bar{v}_{in}}\frac{4}{(2+N_0\omega\Delta z)^2} \times \exp\left[-\frac{2}{(2+N_0\omega\Delta z)}\frac{\upsilon(d)}{\bar{v}_{in}}\right]\mathscr{H}\left[t-\frac{\Delta z}{v_d}\right] \tag{102}$$

7.3.3. Case 3: breakage and coalescence, $d \in [0, 2.7]$

Using the technique reported by Hasseine et al. (2018), we can derive the analytical solution from that developed by McCoy and Madras (2003) for the batch problem, leading to:

$$n(t,z,d) = \upsilon'(d)\frac{N_0}{\bar{v}_{in}}[\Phi(z)]^2\exp\left[-\Phi(z)\frac{\upsilon(d)}{\bar{v}_{in}}\right]\mathscr{H}\left[t-\frac{\Delta z}{v_d}\right] \tag{103}$$

where

$$\Phi(z) = \Phi(\infty)\frac{1+\Phi(\infty)\tanh(\Phi(\infty)\omega\Delta z N_0/2)}{\Phi(\infty)+\tanh(\Phi(\infty)\omega\Delta z N_0/2)}, \quad \Phi(\infty) = \left[\frac{2g_0\bar{v}_{in}}{\omega_0 N_0}\right]^{1/2} \tag{104}$$

For this solution, N_0 and $\bar{v}_{in}$ are constants for all t and z.

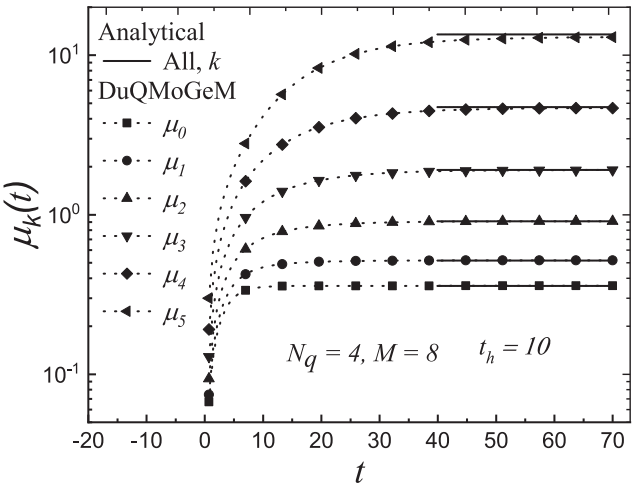

(a)

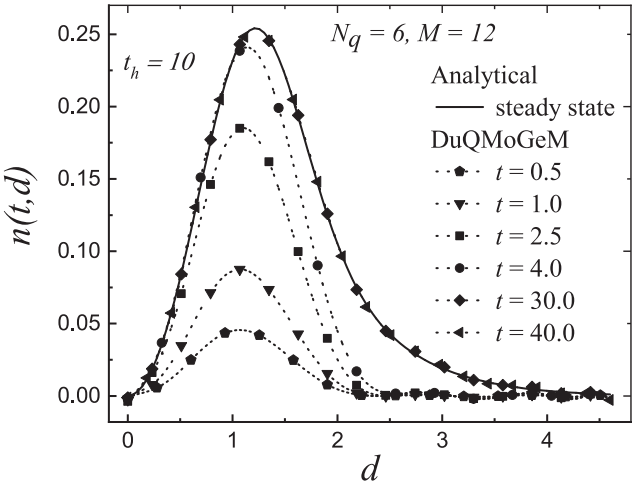

(b)

Fig. 7. Pure coalescence problem in a continuous flow extraction vessel: comparison of the analytical and numerical results.

Table 1
Breakage and coalescence functions.

Case	$B(d/u)$	$g(d) = g_0\upsilon(d)$	$\omega(d,u) = \omega_0$
1	$6d^2/u^3$	$g_0 = 10^{-2}$	$\omega_0 = 0$
2	0	$g_0 = 0$	$\omega_0 = 0.5$
3	$6d^2/u^3$	$g_0 = 1.92 \times 10^{-2}$,	$\omega_0 = 0.3$

7.3.4. Convergence regarding the number of compartments

For $N_q = 3$ and $M = 6$, the effect of the number of compartments in the DuQMoGeM solution for Case 1 was studied for $J = 50, 100$ and 200 compartments. The results for the first four regular moments are presented in Fig. 8, which shows that the DuQMoGeM accuracy improves by increasing the number of compartments. However, $J = 200$ is still not enough to accurately capture the sharp moving front of the solution due to the numerical diffusion of the upwind scheme used for the advective part of F_j.

7.3.5. Prediction of the steady-state solution

Using $N_q = 4, M = 8$ and $J = 100$, the DuQMoGeM steady-state results for the moments of order $k = 1, 2, 3$ and 4 are compared

with the analytical solution for the pure breakage, pure coalesence, and simultaneous breakage and coalescence in Fig. 9. The accuracy of the moments predicted by DuQMoGeM is very good. The third moment, μ_3, is constant after the injection point ($\zeta = 0.1$) in all cases due to the absence of mass transfer.

The numerical and analytical distributions are shown in Fig. 10 at steady state at several ζ points. The DuQMoGeM results were obtained with $N_q = 6, M = 12$ and $J = 100$. The agreement between the simulated and analytical distributions is quite good, showing the ability of the DuQMoGeM to predict the drop number distributions in an extraction column.

Table 2 shows the mean CPU times and their standard deviations computed for 20 runs of case 3 simulation using each one of five sets of values for N_q, M, and J, which were defined as variations of the base case ($N_q = 3, M = 6$ and $J = 100$). When J doubled, the computational cost increased about 2.4 times. A 10-fold increase in M, added 38% in the CPU time. The simulation with $N_q = 3$ is about 67% more costly than that with $N_q = 2$. Therefore, the cost increase with M is mild, but it is superlinear with J or N_q for this simple problem.

7.4. Experimental validation of an extraction column

As a final test, we compared the DuQMoGeM results with the experimental data of Hasseine et al. (2005) for the hydrodynamic behavior of a laboratory-scale Kühni column without mass transfer. It was operated in countercurrent mode with water as the continuous phase and toluene forming the drops of the dispersed phase. Many researchers widely used this chemical system that is recommended by the EFCE (European Federation of Chemical Engineering) as a test system for liquid extraction studies. This column has 44 compartments. The dispersed-phase was fed at compartment five ($j_d = 5$ and $z_d/h = 0.091$), and the continuous phase inlet is at the bottom of compartment 43 ($z_c = 294$ cm). The active height of the column, where there is mechanical agitation, consists of compartments 5 to 41. Table 3 shows the operating conditions and column dimensions, while Table 4 presents the physical properties of both phases. We reported the details of the Kühni column modeling in Appendix A.

The numerical simulation of the Kühni column was carried out with $J = 44$, corresponding to the actual number of stages. We verified the convergence of the results by comparing those obtained using $N_q = 3$ and 4 and $M = 16$ and 32. After some preliminary simulations, we chose $[0.01, 0.4]\,cm$ as the diameter range. Sensitivity of the results to these choices of d_{min} and d_{max} was performed, and the results were essentially the same. Minor differences in the drop Sauter mean diameter results occurred only below the disperse-phase inlet, where the holdup is essentially zero. The simulation reaches the steady-state profiles for the hold up after about 1000 s, but the breakage and coalescence dynamics were much faster. Thus, the results at $t = 1200$ can represent the steady-state. Fig. 11 shows the simulated holdup profile and drop Sauter mean diameter together with the available experimental data (Hasseine et al., 2005). Considering that the Sauter mean diameter data are scattered, the agreement between experimental and simulated data is fairly good. The simulation from $t = 0$ to 1200s

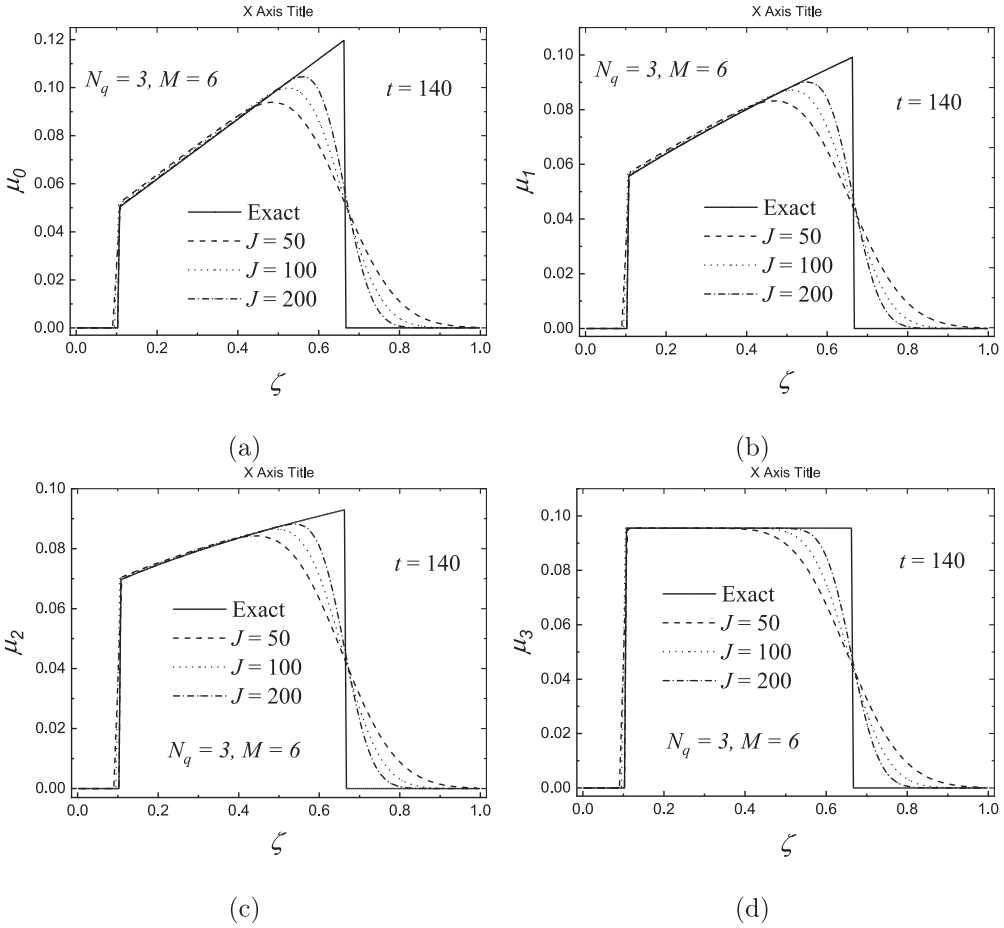

Fig. 8. DuQMoGeM convergence regarding the number of compartments for the pure breakage problem.

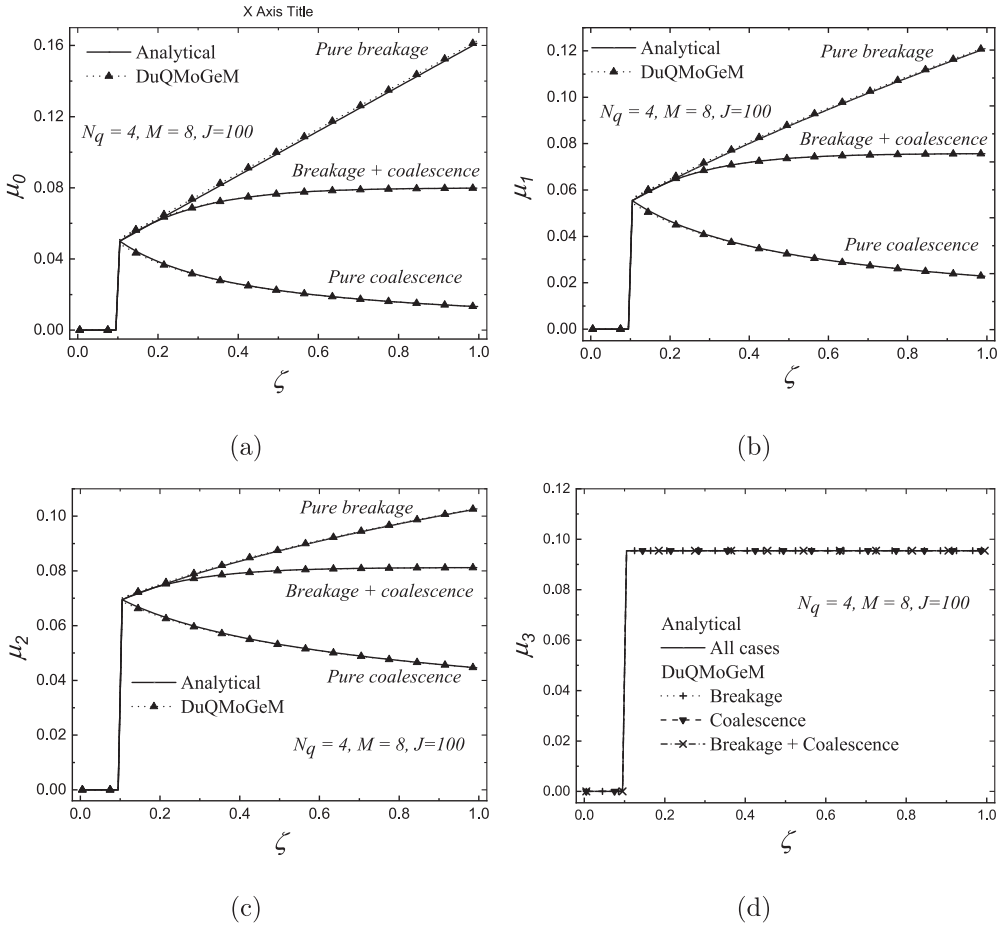

Fig. 9. Comparison of the analytical and numerical moments for steady-state solutions in an extraction column.

whose results are shown in Fig. 11 took about 930 s on an Intel(R) Core(TM) i7-2600 K@3.40 GHz (GNU FORTRAN compiler, version 9.3.0).

8. Conclusion

Population balance models, including breakage and coalescence, were solved using DuQMoGeM for describing the dispersed phase behavior in liquid-liquid dispersed systems.

We analyzed DuQMoGeM solutions for batch and continuous flow well-mixed vessels and liquid-liquid extraction columns. We considered problems including breakage and coalescence for which analytical solutions exist. The moments of the droplet size distribution predicted by the DuQMoGeM were in excellent agreement with the analytical solutions. Besides, the DuQMoGeM approximation for the drop number distribution was also shown to be in good agreement with the analytical solutions.

We modeled and simulated a Kuhni column for which some experimental data exists. The DuQMoGeM results for the disperse phase holdup agreed well with the experimental data at the steady-state, and the simulated drop Sauter mean diameter compared favorably with the scattered experimental data.

Therefore, we showed that the DuQMoGeM is a very efficient technique for solving droplet population balance models, being quite promising for modeling and simulating liquid-liquid extraction columns.

Declaration of Competing Interest

The authors declare that they have no known competing financial interests or personal relationships that could have appeared to influence the work reported in this paper.

Acknowledgments

This work has been partially carried out during a scholarship leave granted to one of the authors (Mr. Khaled Athmani) from the University of Biskra, Algeria, to stay at the Thermofluid Dynamic Laboratory of the Programa de Engenharia Química at COPPE/UFRJ, Brazil, during the academic year 2019/2020. Paulo L. C. Lage acknowledges the financial support from CNPq, Grant Nos. 305276/2019-0 and 305265/2015-6.

Appendix A. Kühni column modeling

A.1. Drop velocity correlations

The drop terminal velocity, v_t, was calculated according to the value of Morton number using the correlations given by Godfrey and Slater (1994), Klee and Treybal (1956), Grace et al. (1976), and Vignes (1965).

The slowing factor values for the Kühni column are provided by (Fang et al., 1995):

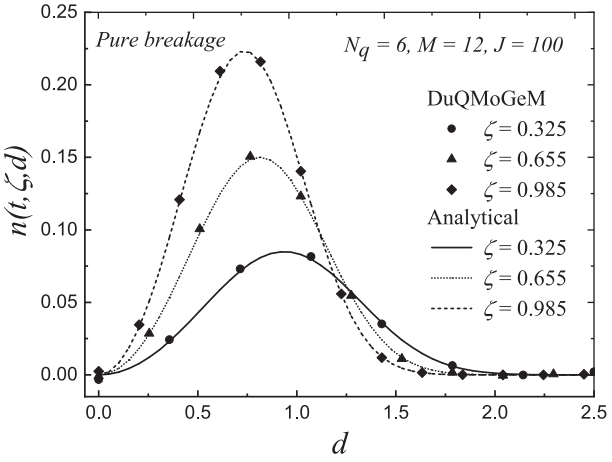

(a)

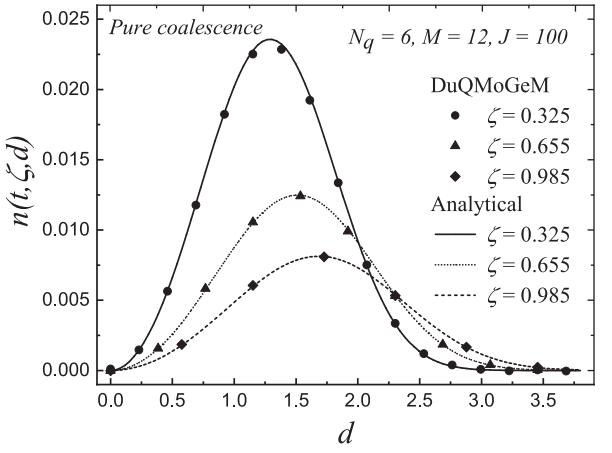

(b)

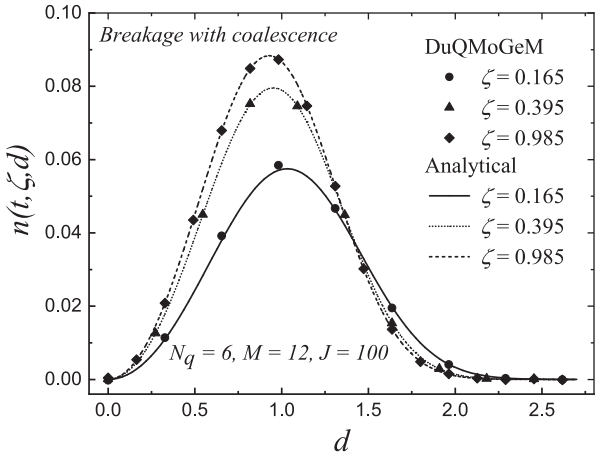

(c)

Fig. 10. Comparison of the analytical and numerical distributions in an extraction column.

Table 2
CPU times for simulating Case 3.*

Conditions	CPU time (s)	Standard deviation (s)
$N_q = 3, M = 6, J = 50$	0.85	0.02
$N_q = 3, M = 6, J = 100$	2.15	0.20
$N_q = 3, M = 6, J = 200$	5.06	0.11
$N_q = 3, M = 60, J = 100$	2.97	0.10
$N_q = 2, M = 6, J = 100$	1.28	0.03

*CodeBlocks 20.03 (Windows 10) on a Intel(R) Core(TM) i3-2348@2.30 GHz.

Table 3
Kühni column parameters.

Turbine diameter	$D_R = 0.085\ m$
Compartment height	$h_j = 0.07\ m, \forall j$
Total height	$h = 3.08\ m$
Active part	$2.52\ m$
Throughput continuous phase	$Q_c = 125\ L/h$
Throughput through the distributor	$Q_d = 130\ L/h$
Column diameter	$D = 0.15\ m$
Energy dissipation	$\epsilon = 0.0788\ W/kg$

$$k_v = 1 - (1-\theta)\left(\frac{7.1810^{-5} Re_R/\theta}{1 + 7.1810^{-5} Re_R/\theta}\right) \tag{A.1}$$

where θ is the relative free cross-sectional stator area and Re_R is defined by:

$$Re_R = \frac{\rho_c D_R^2 N_R}{\eta_c} \tag{A.2}$$

The exponent in the swarm effect term was calculated from Bailes et al. (1986) correlation:

$$\kappa = 4.45 Re_p^{-0.1} - 1, \quad Re_p = \frac{\rho_c d v_t k_v}{\eta_c} \tag{A.3}$$

A.2. Initial and feed conditions

There are no drops in the column at $t = 0$, and the inlet drop distribution n_{in} is the experimental piecewise constant distribution employed by Hasseine et al. (2005), whose mean Sauter diameter is 0.294 cm.

A.3. Dispersion coefficient correlations

We employed the dispersion coefficient correlations given by Steiner et al. (1988). For the continuous phase, the correlation is applied to each compartment:

$$\mathscr{D}_{c,j}(t) = \bar{v}_{c,j} h_j \left[0.188 + 0.0267\theta^{0.5} \frac{D_R N_R}{\bar{v}_{c,j}}\right] \tag{A.4}$$

where $\bar{v}_{c,j} = Q_c/[A(1 - r_{d,j}(t))]$ is the interstitial continuous-phase velocity and h_j is the actual height of the compartment j in the Kühni column. For the disperse phase, Steiner et al. (1988) also provided a correlation, but they recommended its usage with caution:

$$\mathscr{D}_{d,cor} = -3.78 \times 10^{-4} + 0.068 \left[\frac{Q_c}{A N_R}\right]^{0.5} \tag{A.5}$$

Since $\mathscr{D}_d \to \mathscr{D}_c$ from above as the mixing intensity increases (Gourdon et al., 1994), and following Seikova et al. (1992), we used:

$$\mathscr{D}_{d,j}(t) = \max\left(\mathscr{D}_{d,cor}, \mathscr{D}_{c,j}(t)\right) \tag{A.6}$$

Table 4
Chemical system properties.

η_c (mPa)	η_d (mPa)	ρ_c (kg/m^3)	ρ_d (kg/m^3)	σ (mNm^{-1})
0.92	0.6	997.2	862.2	33.7

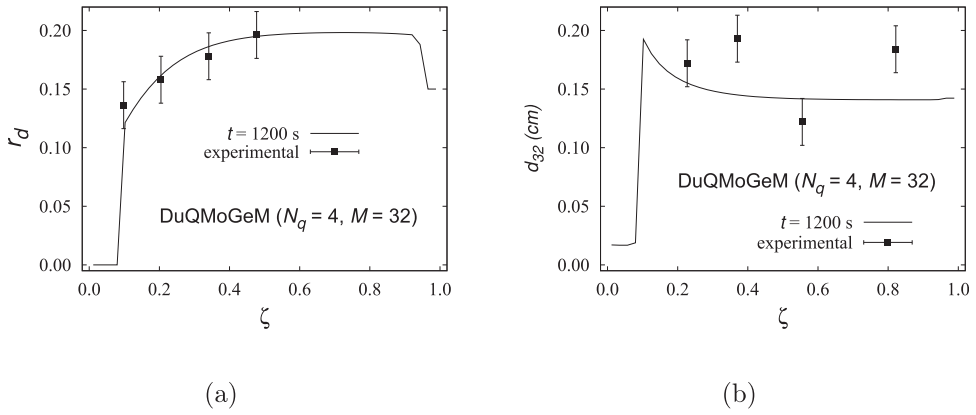

Fig. 11. Simulated and experimental data for the Kühni column at steady-state: (a) dispersed phase holdup and (b) Sauter mean diameter.

It should be noted that $\mathscr{D}_{c,j}$ and $\mathscr{D}_{d,j}$ are assumed null for the non-active sections of the Kühni column.

A.4. Drop breakage

Different breakup mechanisms exist and strongly depend on the column geometry. The drop breakage probability is supposed to be homogeneous in each compartment (Hasseine et al., 2005), the breakage frequency and the breakage probability were modeled by Cauwenberg et al. (1997, 2002) and recommended by Modes (2000):

$$\frac{P(d)}{1-P(d)} = 0.2148 We_m^{0.7796} \tag{A.7}$$

where

$$We_m = \frac{\rho_c^{0.8}\eta_c^{0.2} d D_R^{1.6}(\varpi^{1.8} - \varpi_{crit}^{1.8})}{\sigma} \tag{A.8}$$

where D_R is the rotor diameter. The breakage frequency depends on the residence time:

$$g(z,d) = \frac{P(d)\, v_d(z,d)}{h_j} \tag{A.9}$$

$$\varpi_{crit} = 2\pi 0.65 \left(\frac{\rho_c D_R^3}{\sigma}\right)^{-0.5} \left(\frac{d}{D_R}\right)^{-0.72} \tag{A.10}$$

The daughter droplet size distribution is described by a β distribution, based on the mother drop diameter d_0 (Bahmanyar and Slater, 1991):

$$B(d_0,d) = 3(v-1)\left(1 - \frac{d^3}{d_0^3}\right)^{v-2} \frac{d^2}{d_0^3} \tag{A.11}$$

where the mean number of daughter drops is calculated by:

$$v = 2 + 0.838\left[\left(\frac{d_0}{d_{crit}}\right) - 1\right]^{1.309} \tag{A.12}$$

The critical diameter at which drops start to break is given by:

$$d_{crit} = 0.65 D_R We_R^{-0.72} \tag{A.13}$$

where:

$$We_R = \frac{\rho_c D_R^3 N_R^2}{\sigma} \tag{A.14}$$

A.5. Drop coalescence

For this process, the system properties at interfaces, the intensity of the collision and the contacting time between the colliding drops are key parameters. It is usual to define the coalescence rate as:

$$\omega(d_1,d_2,r_d) = \lambda(d_1,d_2,r_d) f(d_1,d_2,r_d) \tag{A.15}$$

where λ is the collision efficiency, and f is the collision frequency. From the literature (Coulaloglou and Tavlarides, 1977), the expressions for λ and f can be modeled by:

$$\lambda(d_1,d_2,r_d) = \exp\left[-\frac{C_2 \eta_c \rho_c \epsilon \left(\frac{d_1 d_2}{d_1+d_2}\right)^4}{(1+r_d)^3 \sigma^2}\right] \tag{A.16}$$

and

$$f(d_1,d_2,r_d) = \frac{C_1 \sqrt[3]{\epsilon}(d_1+d_2)^2 \sqrt{d_1^{2/3}+d_2^{2/3}}}{1+r_d} \tag{A.17}$$

where ϵ is the specific energy input, $C_1 = 0.01$ and $C_2 = 10^8\, m^{-2} = 10^4\, cm^{-2}$.

A.6. Mechanical power dissipation per unit mass

The power dissipation per unit mass is a parameter that affects the drop behavior in agitated systems (Kumar and Hartland, 1995). The effect of the rotor can be

$$\epsilon = \frac{\mathscr{P}}{\rho_c A h_j} = \frac{4\mathscr{P}}{\pi D^2 h_j \rho_c} \tag{A.18}$$

The power input per compartment can be calculated by:

$$\mathscr{P} = N_p N_R^3 D_R^5 \rho \tag{A.19}$$

where $N_p$is the power number of the column:

$$N_p = 1.08 + \frac{10.94}{Re_R^{0.5}} + \frac{257.37}{Re_R^{1.5}} \tag{A.20}$$

References

Attarakih, M.M., Bart, H.J., Faqir, N.M., 2004. Numerical solution of the spatially distributed population balance equation describing the hydrodynamics of interacting liquid–liquid dispersions. Chem. Eng. Sci. 59, 2567–2592.

Attarakih, M.M., Bart, H.J., Faqir, N.M., 2006. Solution of the population balance equation using the sectional quadrature method of moments (sqmom). Comput. Aided Chem. Eng. 21, 209–214.

Bahmanyar, H., Slater, M.J., 1991. Studies of drop break-up in liquid-liquid systems in a rotating disc contactor. part i: Conditions of no mass transfer. Chem. Eng. Technol. Ind. Chem. Plant Equipment Process Eng. Biotechnol. 14, 79–89.

Bailes, P.J., Gledhill, J., Godfrey, J.C., Slater, M.J., 1986. Hydrodynamic behaviour of packed, rotating disc and kühni liquid/liquid extraction columns. Chem. Eng. Res. Des. 64, 43–55.

Bart, H.J., Jildeh, H., Attarakih, M., 2020. Population balances for extraction column simulations—an overview. Solvent Extr. Ion Exch. 38, 14–65.

Campos, F., Lage, P., 2003. A numerical method for solving the transient multidimensional population balance equation using an euler–lagrange formulation. Chem. Eng. Sci. 58, 2725–2744.

Cauwenberg, V., Degrève, J., Slater, M.J., 1997. The interaction of solute transfer, contaminants and drop break-up in rotating disc contactors: Part i. correlation of drop breakage probabilities. Can. J. Chem. Eng. 75, 1046–1055.

Coulaloglou, C., Tavlarides, L.L., 1977. Description of interaction processes in agitated liquid-liquid dispersions. Chem. Eng. Sci. 32, 1289–1297.

Fang, J., Godfrey, J., Mao, Z.Q., Slater, M., Gourdon, C., 1995. Single liquid drop breakage probabilities and characteristic velocities in kühni columns. Chem. Eng. Technol. 18, 41–48.

Garthe, D., 2006. Fluiddynamics and mass transfer of single particles and swarms of particles in extraction columns Ph.D. thesis. Technische Universität München.

Gautschi, W., 1994. Algorithm 726: ORTHPOL — A Package of Routines for generating Orthogonal Polynomials and Gauss-Type Quadrature Rules. ACM Trans. Math. Softw. 20, 21–62.

Gayler, R., Roberts, N., Pratt, H.R., 1953. Liquid-Liquid Extraction. Part 4. A Further Study of Hold-up in Packed Columns. Technical Report. Atomic Energy Research Establishment, Harwell, Berks (England).

Gelbard, F., Seinfeld, J.H., 1978. Numerical solution of the dynamic equation for particulate systems. J. Comput. Phys. 28, 357–375.

Godfrey, J.C., Slater, M.J., 1994. Liquid-liquid extraction equipment. Wiley, New York.

Gourdon, C., Casamatta, G., Muratet, G., 1994. Population balance based modelling. In: Godfrey, J., Slater, M. (Eds.), Liquid-Liquid Extraction Equipment. John Wiley & Sons, New York, pp. 141–226.

Grace, J., TH, N., et al., 1976. Shapes and velocities of single drops and bubbles moving freely through immiscible liquids. Chem. Eng. 54, 167–173.

Hasseine, A., Athmani, K., Bart, H.J., 2018. Variational iteration method and projection method solution of the spatially distributed population balance equation. Arab J. Basic Appl. Sci. 25, 132–141.

Hasseine, A., Hlawitschka, M.W., Omar, W., Bart, H.J., 2020. New analytical and numerical solutions of the particle breakup process. Open Chem. Eng. J. 14.

Hasseine, A., Meniai, A.H., Lehocine, M.B., Bart, H.J., 2005. Assessment of drop coalescence and breakup for stirred extraction columns. Chem. Eng. Technol. Ind. Chem. Plant Equipment-Process Eng. Biotechnol. 28, 552–560.

Hounslow, M.J., 1990. A discretized population balance for continuous systems at steady state. AIChE J. 36, 106–116.

Hulburt, H.M., Katz, S., 1964. Some problems in particle technology: A statistical mechanical formulation. Chem. Eng. Sci. 19, 555–574.

John, V., Angelov, I., Öncül, A., Thévenin, D., 2007. Techniques for the reconstruction of a distribution from a finite number of its moments. Chem. Eng. Sci. 62, 2890–2904.

Klee, A.J., Treybal, R.E., 1956. Rate of rise or fall of liquid drops. AIChE J. 2, 444–447.

Kronberger, T., Ortner, A., Zulehner, W., Bart, H.J., 1995. Numerical simulation of extraction columns using a drop population model. Comput. Chem. Eng. 19, 639–644.

Kumar, A., Hartland, S., 1995. A unified correlation for the prediction of dispersed-phase hold-up in liquid-liquid extraction columns. Ind. Eng. Chem. Res. 34, 3925–3940.

Kumar, S., Ramkrishna, D., 1996a. On the solution of population balance equations by discretization—i. a fixed pivot technique. Chem. Eng. Sci. 51, 1311–1332.

Kumar, S., Ramkrishna, D., 1996b. On the solution of population balance equations by discretization—ii. a moving pivot technique. Chem. Eng. Sci. 51, 1333–1342.

Kumar, S., Ramkrishna, D., 1997. On the solution of population balance equations by discretization—iii. nucleation, growth and aggregation of particles. Chem. Eng. Sci. 52, 4659–4679.

Lage, P.L., 2011. On the representation of qmom as a weighted-residual method—the dual-quadrature method of generalized moments. Comput. Chem. Eng. 35, 2186–2203.

Mantzaris, N.V., Daoutidis, P., Srienc, F., 2001a. Numerical solution of multi-variable cell population balance models: I. finite difference methods. Comput. Chem. Eng. 25, 1411–1440.

Mantzaris, N.V., Daoutidis, P., Srienc, F., 2001b. Numerical solution of multi-variable cell population balance models. iii. finite element methods. Comput. Chem. Eng. 25, 1463–1481.

Marchisio, D.L., Fox, R.O., 2005. Solution of population balance equations using the direct quadrature method of moments. Aerosol Sci. 36, 43–73.

Marchisio, D.L., Vigil, R.D., Fox, R.O., 2003. Quadrature method of moments for aggregation-breakage processes. J. Colloid Interface Sci. 258.

McCoy, B.J., Madras, G., 2003. Analytical solution for a population balance equation with aggregation and fragmentation. Chem. Eng. Sci. 58, 3049–3051.

McGraw, R., 1997. Description of aerosol dynamics by the quadrature method of moments. Aerosol Sci. Technol. 27, 255–265.

Modes, G., 2000. Grundsätzliche Studie zur Populationsdynamik einer Extraktionskolonne auf Basis von Einzeltropfenuntersuchungen. Shaker.

Nicmanis, M., Hounslow, M., 1996. A finite element analysis of the steady state population balance equation for particulate systems: Aggregation and growth. Comput. Chem. Eng. 20, S261–S266.

Petzold, L., 1982. A description of DASSL: A differential/algebraic system solver. Technical Report. Sandia National Laboratories.

Ramkrishna, D., 2000. Population Balances — Theory and Applications to Particulate Systems in Engineering. Academic Press, San Diego.

Santos, F., Favero, J., Lage, P., 2013. Solution of the population balance equation by the direct dual quadrature method of generalized moments. Chem. Eng. Sci. 101, 663–673.

Seikova, I., Gourdon, C., Casamatta, G., 1992. Single-drop transport in a kühni extraction column. Chem. Eng. Sci. 47, 4141–4154.

Simon, M., Schmidt, S., Bart, H.J., 2002. Bestimmung von zerfalls-und koaleszenzparametern in flüssig/flüssig-systemen auf der grundlage von einzeltropfenexperimenten. Chem. Ing. Tech. 74, 247–256.

Steiner, L., Kumar, A., Hartland, S., 1988. Determination and correlation of axial-mixing parameters in an agitated liquid-liquid extraction column. Can. J. Chem. Eng. 66, 241–247.

Su, J., Gu, Z., Xu, X.Y., 2009. Advances in numerical methods for the solution of population balance equations for disperse phase systems. Sci. China Ser. B: Chem. 52, 1063–1079.

Vignes, A., 1965. Hydrodynamique des dispersions. Genie Chimique 93, 129–142.

Weber, B., Schneider, M., Görtz, J., Jupke, A., 2020. Compartment model for liquid-liquid extraction columns. Solvent Extr. Ion Exch. 38, 66–87.

Yuan, C., Laurent, F., Fox, R., 2012. An extended quadrature method of moments for population balance equations. J. Aerosol Sci. 51, 1–23.